MODELING AND ANALYSIS OF A COMPOSITE B-PILLAR FOR SIDE-IMPACT PROTECTION OF OCCUPANTS IN A SEDAN

A Thesis by

Santosh Reddy

Bachelor of Engineering, VTU, India, 2003

Submitted to the College of Engineering
and the faculty of Graduate School of
Wichita State University
in partial fulfillment of
the requirements for the degree of
Master of Science

May 2007

MODELING AND ANALYSIS OF A COMPOSITE B-PILLAR FOR SIDE-IMPACT PROTECTION OF OCCUPANTS IN A SEDAN

I have examined the final copy of thesis for form and content and recommend that it be accepted in partial fulfillment of the requirements for the degree of Master of Science, with a major in Mechanical Engineering.

_____
Hamid M. Lankarani, Committee Chair

We have read this thesis and recommend its acceptance

_____
Kurt soschinske, Committee Member

_____
M.Bayram Yildirim, Committee Member

DEDICATION

To My Parents & Sister

ACKNOWLEDGEMENTS

I would like to express my sincere gratitude to my graduate advisor, Dr. Hamid M. Lankarani, who has been instrumental in guiding me towards the successful completion of this thesis. I would also like to thank Dr. Kurt Soschinske and Dr. M. Bayram Yildirim for reviewing my thesis and making valuable suggestions.

I am indebted to National Institute for Aviation Research (NIAR) for supporting me financially throughout my Master's degree. I would like to acknowledge the support of my colleagues at NIAR, especially the managers Thim Ng, Tiong Keng Tan and Kim Leng in the completion of this thesis.

Special thanks to Ashwin Sheshadri, Kumar Nijagal, Arun Kumar Gowda, Siddartha Arood, Krishna N Pai, Anup Sortur, ShashiKiran Reddy, Sahana Krishnamurthy, Praveen Shivalli, Geetha Basavaraj, Akhil Kulkarni, Sir Chin Leong, Evelyn Lian, Arvind Kolhar in encouragement and suggestions throughout my Masters degree.

I also extend my gratitude to my parents, sister, cousins and all my friends who stood by me at all times.

ABSTRACT

Cars safety became an issue almost immediately after the invention of the automobile. To protect occupants from a direct impact, the passenger compartment and the structure of the vehicle should keep its shape in a crash. Continuous developments to improve is proposed everyday, standards are set in pertinent to different crash scenarios such as the frontal crash, side impact and so on. Among these standards, side impact is one of the most fatal crash scenarios that lead to death of people in the United States and across the globe. In the contemporary world, fuel consumption also poses a serious issue that has to be considered. With these constraints in consideration, a lighter and stronger material than steel, the composite material, can be used. Using this material would help in reducing the fuel efficiency without sacrificing the safety of the vehicle.

With the advance in computer simulations, finite element (FE) model of the Ford Taurus and Moving Deformable Barrier (MDB) developed by the National Crash Analysis Center (NCAC) has been used for different impact scenarios to predict the vehicle behavior and occupant response. In addition, MSC Patran has been used as the modeler and LS-Dyna as the solver to run the required simulations. MADYMO is used to predict the injury parameters.

In this research, a composite B-Pillar that is the energy absorbing structure is modeled and analyzed with Finite Element Analysis. The injuries sustained by the occupant are predicted using Madymo. An attempt is made to use carbon and glass fiber composite materials in the B-Pillar modeled in this study. In addition, a parametric study is carried out on the B-Pillar to determine the maximum possible energy absorbing parameters. It is demonstrated that the new modeling with the use of carbon/glass with a

pertinent orientation and thickness may present more energy absorption than the present steel pillar. Energy absorption, displacement and the acceleration of the present and the new model are also compared and discussed in detail. Occupant injuries, such as chest and head injuries are compared for the vehicle occupants with present and the new model. It is demonstrated that the new B-Pillar composite model with carbon may be more effective than the present steel pillar.

TABLE OF CONTENTS

TABLE OF CONTENTS (Continued)

Chapter Page

TABLE OF CONTENTS (Continued)

Chapter Page

LIST OF FIGURES

LIST OF FIGURES (Continued)

LIST OF TABLES

LIST OF SYMBOLS

ρ	Density of the structure material
$\bar{\sigma}$	Average collapse shear
δ	Deformed length
$\bar{F}$	Average collapse load
ω	Angular velocity
V_{node}	Nodal velocity
V_{cm}	Velocity at the center of mass
μ	Viscosity coefficient
G	Elastic shear modulus
λ	Strain rate

CHAPTER 1

INTRODUCTION

1.1 Motivation

Development of automotive structures to sustain impact loading in diverse crash conditions such as, frontal perpendicular, angular, offset, pole impacts and side collisions are required. In addition, other non-crash functional requirements, such as, vibration, durability and fatigue life cycle are also integral part of vehicle design. However, with growing focus on safety new vehicles are expected to be crash tested under newer and more demanding crash conditions, such as, the vehicle-to-vehicle 30-degree oblique offset impact under consideration by National Highway Traffic Safety Administration [1]. This shift may result into body structure designs with higher strength, stiffness and higher mass. At the same time environmental and fuel economy requirements dictate that vehicle design be lighter and compact resulting in smaller crush space. When crush space is limited, the body structure, typically designated to dissipate major share of impact energy, require thicker sheet metal and/or higher strengths alloys translating to added weight.

1.2 Crashworthiness

The ability of the vehicle to absorb energy and to prevent occupant injuries in the event of an accident is referred to as “Crashworthiness” [2]. The vehicle must be designed such that, at higher speeds its occupants do not experience a net deceleration greater than 20 g. Crashworthiness can be categorized into three basic areas, materials engineering and design, combustion and fire and finally medical engineering (biomechanics). It covers civil, automotive, military, marine and aerospace oriented

applications, where the automotive sector is probably the most prominent area in this respect. Crashworthiness features includes air bags, seat belts, crumple zones, side impact protection, interior padding and headrests. These features are updated when there is a new safer and better design [2].

Crashworthiness is not the same as vehicle safety, and the two topics must be distinguished. The safety of a vehicle depends on crashworthiness and as well as the accident avoidance features, which might include ABS, good handling characteristics, or even oversize tires. One vehicle might be safer statistically than another and still have a significant crashworthiness defect. It could even conceivably be less crashworthy overall while still being a "safer" vehicle.

Structural crashworthiness involves absorption of kinetic energy by considering designs and materials suitable for controlled and predictive energy absorption. In this process, the kinetic energy of the colliding bodies is partly converted into internal work of the bodies involved in the crash. Crash events are non-linear and may involve material failure, global and local structural instabilities and failure of joints. In addition, strain-rate and inertia effects may play an important role in the response of the structures involved.

Crashworthiness of a material is expressed in terms of its specific energy absorption, $E_s = F/D$, where D is the density of the composite material and F is the mean crush stress. In order to protect passengers during an impact, a structure based on strength and stiffness is far from being optimal. Rather, the structure should collapse in a well-defined deformation zone and keep the forces well below dangerous accelerations. However, since the amount of absorbed energy equals the area under the load deflection curve, the two above mentioned criteria are somewhat contradictory, thus showing that, it

is not only important to know how much energy is absorbed but also how it is absorbed, i.e., how inertia loads are transferred from impact point to panel supports. Therefore, in addition to designing structures able to withstand static and fatigue loads, structures have to be designed to allow maximum energy absorption during impact.

1.2.1 Composite Materials in Crashworthiness

The fuel efficiency and gas emission regulation of the car are also very important in the contemporary world. Every day the price of the fuel and the requirement of the fuel is increasing randomly, eventually emission of chemicals from the vehicle exhaust pollute the environment and increase the global temperature [3]. Composite materials help in reducing the weight of the structure thus bringing down the fuel used.

Composites are engineered materials that have been designed to provide significantly higher specific stiffness and specific strength (stiffness or strength divided by material density)—that is, higher structural efficiency—relative to previously available structural materials. In composite materials, strength and stiffness are provided by the high-strength, high-modulus reinforcements.

Composite materials offer a high potential for tailored designs by a wide variety of matrices and fibers, various performs, and laminate architecture; i.e. fiber orientation and stacking sequence of single laminate. Composite materials also have a considerable potential for absorbing kinetic energy during crash [6]. The composite energy absorption capability offers a unique combination of reduced structural weight and improved vehicle safety by higher or at least equivalent crash resistance compared to metal structures. Crash resistance covers the energy absorbing capability of crushing structural parts as

well as the demand to provide a protective shell around the occupants (structural integrity) [3].

In the last decade, several studies have demonstrated the ability of composite materials to absorb energy under crashworthy conditions. Some of the energy absorbing composite materials structural concepts that have been studied experimentally, especially for this application, include honeycomb sandwich, sine wave web and foam filled stiffened beams. Effects of various material characteristics like ply orientation, stacking sequence, fiber and matrix properties have been investigated and reported. However, different fiber/matrix systems and different geometrical shapes produce substantially different crushing response [6]. Moreover, due to the complex failure behavior, energy absorption and crush/crash behavior of composite structures, there has been a lack of experience when compared with the metallic structures. In this context, extensive tests are typically used to guarantee the crashworthiness of composite structures and to understand the mechanism of energy absorption and failure. The specific energy absorption, post-crushing integrity and energy release of the candidate materials must be known to match specific design requirements. The specific energy absorption for composites is a function of material properties constituting their fiber and matrix, as well as their ply orientation, whereas for metals it is primarily a function of only their plastic behavior. To a limited extent, specimen geometry and material property effects have been reported.

The cost of conducting a crashworthy structure development program is high and as a reason the use of Finite Element Analysis for simulating the response of composite structures under impact and crash loads is preferred. To date, finite element analyses of

composite structures for crashworthiness rely heavily on experimental data. This means that the testing of composite structures or specimens will continue for determining energy absorption behavior [6].

Similarly, due to the high cost and high computational time involved in modeling large structures, finite element analysis is carried out for simulating the crash response of semi-scale structures and specimens. Hybrid finite element models are used to conduct crash analysis of full-scale structures and, to compensate the high computational time.

1.3 Crash Statistics

In the present day accidents happen every hour around the world and most of these are very dangerous. Side-Impact crash is the second most severe crash scenario after frontal-impact. Figure 1 shows the comparison of different crash scenarios involved. It can be observed that the frontal impact is higher than the side-impact. However, the space required for any structure in the event of a side-impact to absorb energy is very less than the frontal-impact. The occupant injuries in the side-impact crash are severe when compared with the frontal crash. Other crashes involved are the rollover and rear impact. These amounts to a lesser crash scenario than the side or the frontal crash [4].

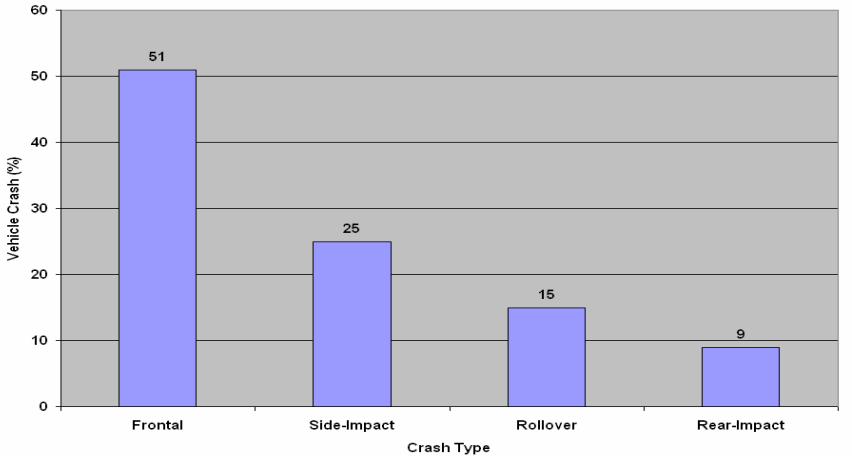

Figure 1. Crash types [4]

Many researchers have carried out extensive study on frontal and side impact crash analysis and have been successful in reducing the risk of the injuries sustained by the occupant. From figure 2, it can be seen that over the past two decades the research on frontal impact has helped in reducing injuries, however, the injuries involved in the event of a side impact crash has increased [4].

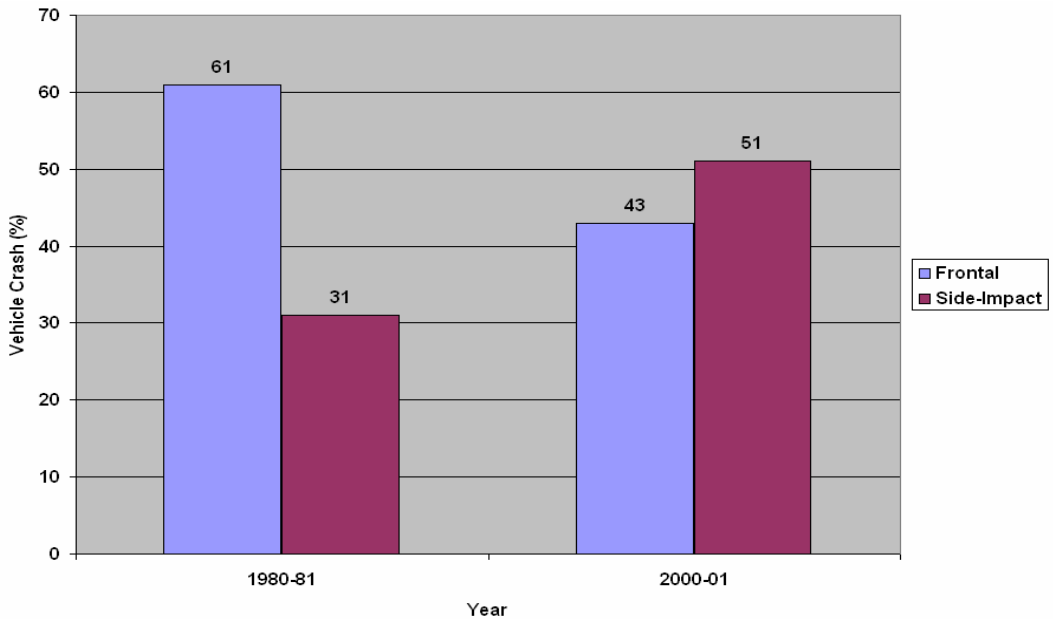

Figure 2. Comparison of frontal and side impact crash [4]

1.4 Test Methodologies

There are different methodologies that can be carried out in a crash test [6].

1.4.1 Quasi-static Testing

In quasi-static testing, the test specimen is crushed at a constant speed. Quasi-static tests may not be an actual simulation of the crash condition because in an actual crash condition, the structure is subjected to a decrease in crushing speed, from an initial impact speed, finally to rest.

The following are some advantages of quasi-static testing.

- Quasi-static tests are simple and easy to control.

- To follow the crushing process, Impact tests require very expensive equipment, as the whole process occurs in a split second. Hence, quasi-static tests are used to study the failure mechanisms in composites, by selection of appropriate crush speeds.

The following is a major disadvantage of quasi-static testing.

- Quasi-static tests may not be a true simulation of the actual crash conditions since certain materials are strain rate sensitive.

1.4.2 Dynamic Collision Test (FMVSS 214)

In this test procedure, a deformable barrier mounted on a sled impacts a car side door angularly. That is, all four wheels of the barrier-sledge are inclined at an angle of 27°. In the front, an aluminum honeycomb barrier is fixed and this is at the height of the bumper so that the real simulation of crash is simulated. Inside the vehicle, a US-Side Impact Dummy is placed on the front seat and this dummy measures the Injury levels sustained [9].

1.4.3 Composite Test Procedure (CTP) for Vehicle Side Impact Testing

As the terminology could imply, this test procedure is not only for a composite. This test starts with the displacement of the barrier into the side of the vehicle until the inner door is in contact with the dummy. At this point, the barrier face is half in this position until the inner wall of the door is loaded using the body forms. Sufficient force-deflection data is obtained for the computer model [10]. After full retraction of the body forms, the barrier face is then deformed further into the side structure of the vehicle and unloaded. Once again, the amount of intrusion is such that suitable force-deflection characteristics of the vehicle side structure ate obtained.

1.4.4 Impact Testing

The crushing speed decreases from the initial impact speed to rest as the specimen absorbs the energy.

The following is a major advantage of impact testing

- It is a true simulation of the crash condition since it takes into account the stress rate sensitivity of materials.

The following is a major disadvantage of impact testing.

- In Impact testing, the crushing process takes place in a fraction of a second. Therefore, it is recommended that crushing be studied with high-speed camera [4].

1.4.5 Crushing Modes and Mechanisms

1.4.5.1 Catastrophic Failure Modes

Catastrophic failure modes are not of interest to the design of crashworthy structures. This type of failure occurs because of the following events:

- When unstable intralaminar or interlaminar crack growth occurs.
- In long thin walled tubes because of column instability.
- In tubes composed of brittle fiber reinforcement, when the lamina bundles do not bend or fracture due to interlaminar cracks being less than a ply thickness.

Catastrophic failure is characterized by a sudden increase in load to a peak value followed by a low post failure load. When unstable interlaminar or interlaminar growth occurs, there is a catastrophic failure. As a result of this, the actual magnitude of energy absorbed is much less and the peak load is too high to prevent injury to the passengers [2].

1.4.5.2 Progressive Failure Modes

Progressive failure can be achieved by providing a trigger at one end. This initiates a failure at a specific location within the structure. The most widely used method of triggering is to chamfer one end of the tube. A number of trigger geometries such as bevels, grooves and holes that have been investigated in laboratory specimens are not as easy to use in vehicle structures

The following are the advantages of progressive failure in the design of crashworthy structures.

- The energy absorbed in progressive crushing is larger than the energy absorbed in catastrophic failure.
- A structure designed to react to loads produced by progressively failing energy absorbers are lighter than structures designed to react to loads produced by catastrophically failing energy absorbers [2].

The following are the different types of progressive failure modes:

1.4.5.3 Transverse Shearing or Fragmentation Mode

- The fragmentation mode is characterized by a wedge-shaped laminate cross section with one or multiple short interlaminar and longitudinal cracks that form partial lamina bundles (Figure 3).
- Brittle fiber reinforcement tubes exhibit this crushing mode.
- The main energy absorption mechanisms is fracturing of lamina bundles.
- When fragmentation occurs, the length of the longitudinal and interlaminar cracks is less than that of the lamina which helps in the transverse shearing or fragmentation mode.

- Mechanisms like interlaminar crack growth and fracturing of lamina bundles control the crushing process for fragmentation [2].

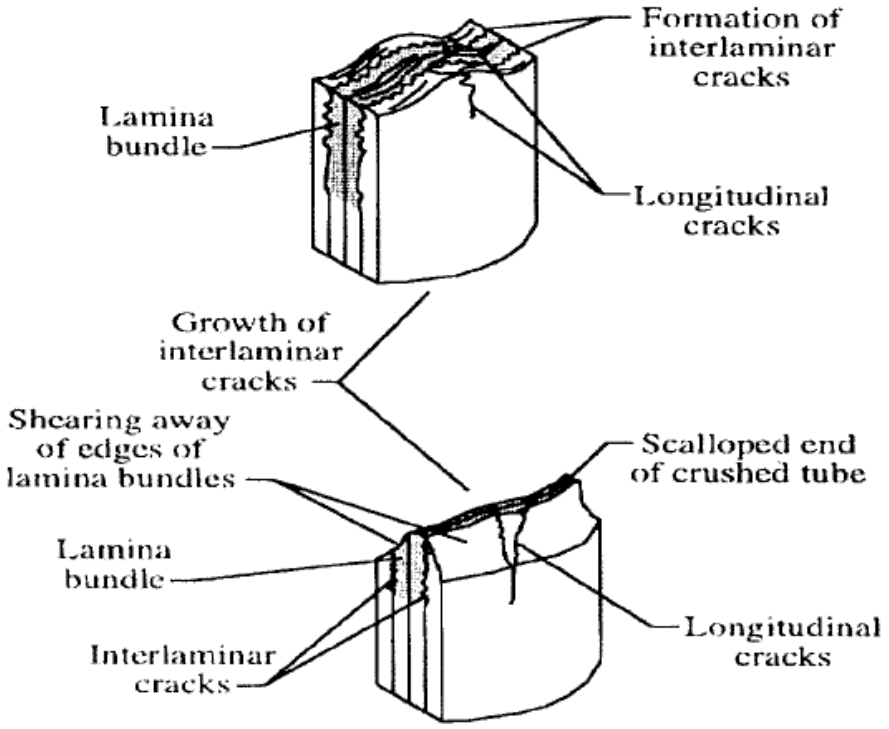

Figure 3. Fragmentation crushing mode [2]

1.4.5.4 Lamina Bending or Splaying Mode

- Very long interlaminar, intralaminar, and parallel to fiber cracks characterizes the splaying mode. The lamina bundles do not fracture. (Figure 4)
- Brittle fiber reinforcement tubes exhibit this crushing mode.
- The main energy absorbing mechanism is matrix crack growth. Two secondary energy absorption mechanisms related to friction occur in tubes that exhibit splaying mode.
- Mechanisms like interlaminar, intralaminar and parallel to fiber crack growth control the crushing process for splaying.

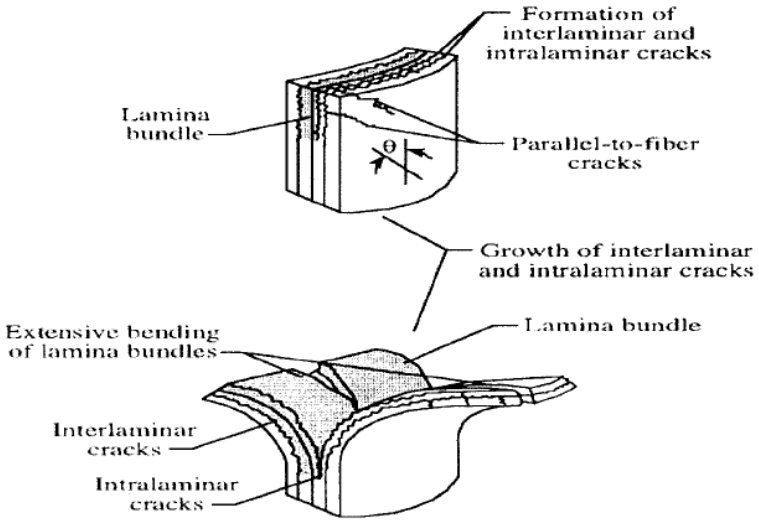

Figure 4. Splaying crushing mode [2]

1.4.5.5 Brittle Fracturing

- The brittle fracturing crushing mode is a combination of fragmentation and splaying crushing modes (Figure 3).
- Brittle fiber reinforcement tubes exhibit this crushing mode.
- The main energy absorption mechanism is fracturing of lamina bundles.
- When brittle fracturing occurs, the lengths of the interlaminar cracks are between 1 and 10 laminate thickness.

1.4.5.6 Local Buckling or Progressive Folding

- The progressive folding mode is characterized by the formation of local buckles (Figure 4).
- This mode is exhibited by both brittle and ductile fiber reinforced composite material.
- Mechanisms like plastic yielding of the fiber and/or matrix control the crushing process for progressive folding [2].

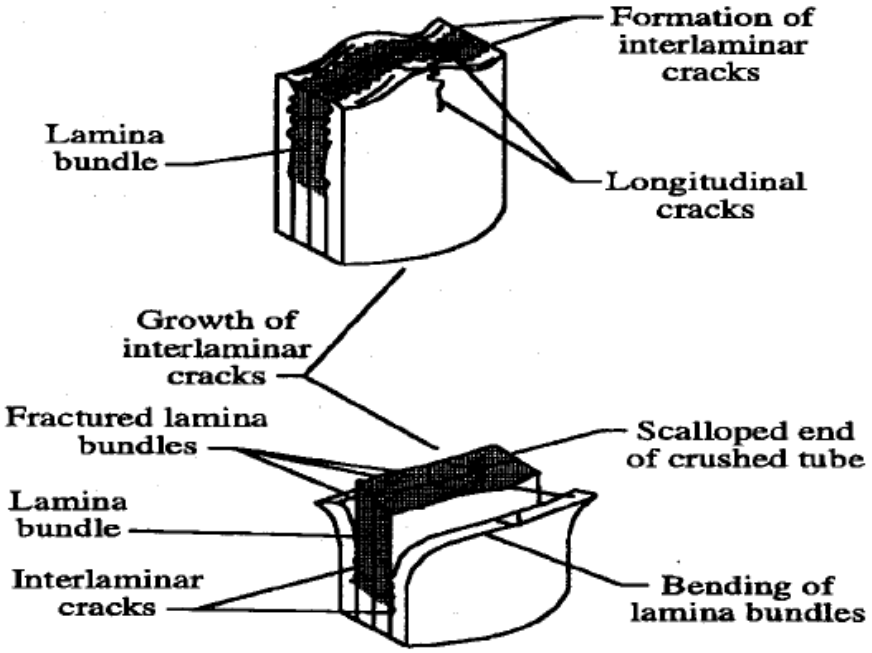

Figure 5. Brittle fracturing crushing mode [5]

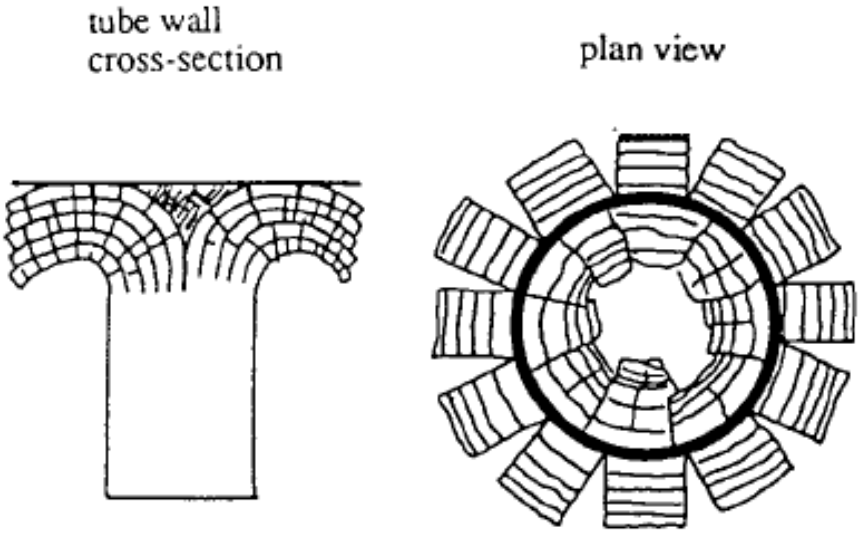

Figure 6. Progressive crushing mode [5]

1.5 Injury Criteria

An injury criterion can be defined as a biomechanical index of exposure severity, which indicates the potential for impact induced injury by its magnitude. There are several kinds of injury criteria's that are related to the human body. These are basically the impact loads acting on the human body. Some of the criteria's pertinent to the Side Impact are discussed here.

1.5.1 Head Injury Criterion (HIC)

The Head Injury Criteria is defined as:

$$HIC = \max_{T0 \le t_1 \le t_2 \le TE} \left[\frac{1}{t_2 - t_1} \int_{t_1}^{t_2} R(t)dt \right]^{2.5} (t_2 - t_1) \tag{1.1}$$

where T0 = start time of simulation

TE = end time of simulation

R(t) = is the resultant head acceleration in g's measured at head's center of gravity over the time interval $T0 \le t \le TE$

t_1 and t_2 are the initial and final times (in sec) of the interval during which the HIC attains a maximum value [16].

A value of 623 is specified as good for the HIC as concussion tolerance level in side (contact) impact. Table 13 shows the injury ratings according to insurance institute for highway safety. For practical reasons, the maximum time interval t2-t1 that is considered to give appropriate head injury criteria values was set to 36 ms. This time interval greatly affects the head injury criteria calculations, and recently this time interval has been proposed to be further reduced to 16 ms in order to restrict the use of HIC to hard head contact impacts.

1.5.2 Thoracic Trauma Index (TTI)

The TTI is the acceleration criterion based on accelerations of the lower thoracic spine and the ribs. The thoracic trauma index (TTI) provides an indication of the severity of injuries received by motor vehicle occupants in side-impact collision environments. It is the method of quantifying the anatomical extent of the injury, which includes injuries to intrathoracic organs. The TTI can be used as an indicator for the side impact performance of passenger cars. The specific benefit of the TTI is that it can be used to address the entire population of vehicle occupants because the age and the weight of the cadaver are included. The TTI is defined by Morgan: [24]

$$TTI = 1.4 * AGE + 0.5 * \left(RIB_g + T12\ \right) * MASS/MSTD \tag{1.2}$$

Where AGE = age of the test subject in years,

RIB_g = maximum absolute value of acceleration in g's of the 4^{th} and 8^{th} rib on the struck side,

$T12_g$ = maximum absolute acceleration values in g's of the 12^{th} thoracic vertebra, in lateral direction,

MASS = test subject mass in kg

MSTD = standard reference mass of 75 kg.

There is also a definition for the TTI that could be used for dummies without a specific age, called the TTI (d). It is defined for 50^{th} percentile dummies with a mass of 75 kg:

$$TTI(d) = 0.5 * \left(RIB_g + T12_g\right) \tag{1.3}$$

The dynamic performance requirement, as stated in FMVSS 214 regulations of 1990, is that the TTI (d) level shall not exceed 85 g for passenger cars with four side doors and 90 g for two side doors.

1.5.3 Viscous Injury Response (V^*C)

The Viscous Response, denoted as V^*C (3), is the maximum value of a time function formed by the product of velocity of deformation (V) and the instantaneous compression function (C): [16]

$$V * C = \max\left(\frac{dD(t)}{dt} \frac{D(t)}{SZ} \right) \tag{1.4}$$

where D (t) is deflection and SZ is prescribed size (the initial torso thickness for frontal impacts or half the torso width for side impacts). Analysis of data from experiments on human cadavers show that a frontal impact which produces a V^*C value of 1m/s has a 50% chance of causing severe thoracic injuries (AIS $\geq$ 4).

1.6 NHTSA/Standard

The National Highway Traffic Safety Administration (NHTSA), under the U.S. Department of Transportation, was established by the Highway Safety Act of 1970, as the successor to the National Highway Safety Bureau, to carry out safety programs under the National Traffic and Motor Vehicle Safety Act of 1966 and the Highway Safety Act of 1966. The Vehicle Safety Act has subsequently been recoded under Title 49 of the U. S. Code in Chapter 301, Motor Vehicle Safety. NHTSA also carries out consumer programs established by the Motor Vehicle Information and Cost Savings Act of 1972, which has been recoded in various Chapters under Title 49. NHTSA is responsible for reducing deaths, injuries and economic losses resulting from motor vehicle crashes. This is accomplished by setting and enforcing safety performance standards for motor vehicles and motor vehicle equipment, and through grants to state and local governments to enable them to conduct effective local highway safety programs. NHTSA investigates safety defects in motor vehicles, sets and enforces fuel economy standards, helps states and a

local community reduce the threat of drunk drivers, promote the use of safety belts, child safety seats and air bags, investigate odometer fraud, establish and enforce vehicle anti-theft regulations and provides consumer information on motor vehicle safety topics. NHTSA also conducts research on driver behavior and traffic safety, to develop the most efficient and effective means of bringing about safety improvements.

Federal Motor Vehicle Safety Standard (FMVSS) 214 (Figure 7), "Side Impact Protection" was amended in 1990 to assure occupant protection in a dynamic test that simulates a severe right-angle collision. It is one of the most important and promising safety regulation issued by the National Highway Traffic Safety Administration (NHTSA). It was phased into new passenger cars during model years 1994-97. In 1993, side impacts accounted for 33 percent of the fatalities to passenger car occupants [9].

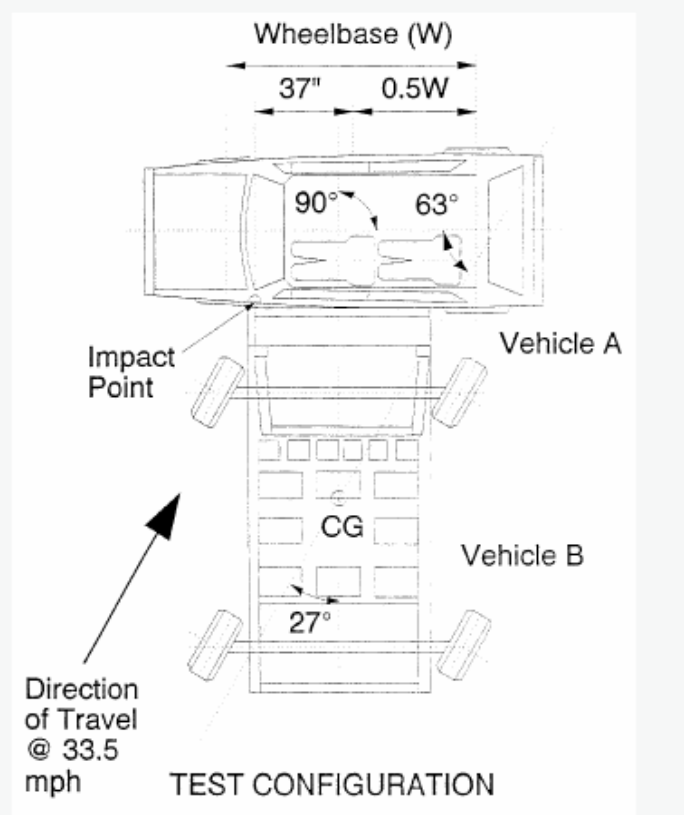

Figure 7. FMVSS 214 test configuration [9]

- A test configuration using a Moving Deformable Barrier (MDB) simulating a severe intersection collision between two passenger vehicles.
- Injury criteria, Thoracic Trauma Index (TTI) that predicts the severity of thoracic injuries when occupant's torsos contact the interior side surfaces of a car.
- A Side Impact Dummy (SID) on which TTI could be reliably measured in side impact tests. The injury score measured on the dummy is called TTI.
- The new FMVSS 214, allowing TTI upto 90 in 2-door cars and 85 in 4-doors cars.

The Government Performance and Results Act of 1993 and Executive Order 12866 require various agencies and automobile manufacturers to evaluate their existing programs and regulations. The objectives of an evaluation are to determine the actual benefits – lives saved, injuries prevented, and damages avoided – and costs of safety equipment installed in production vehicles in connection with a rule [9].

1.7 B-Pillar

B-pillars are one of the most sophisticated parts of the automobile body, because this component has to comply with lot of requirements and specifications. Figure 8 shows the position of B-Pillar in a car. There are 2 parts in the B-Pillar, one is the outer layer and the other is the inner layer. These two layers are made of steel and they are welded together [12]. The distance between the B-Pillar and the occupant is very less in side impact when compared to the frontal impact. In addition, when the impact occurs, the B-Pillar or structures in the B-Pillar have to absorb more energy with minimal acceleration. Since the distance between the B-Pillar and the occupant is very less care has to be taken in the design and manufacture of the B-Pillar. Safety is the main concern in this design.

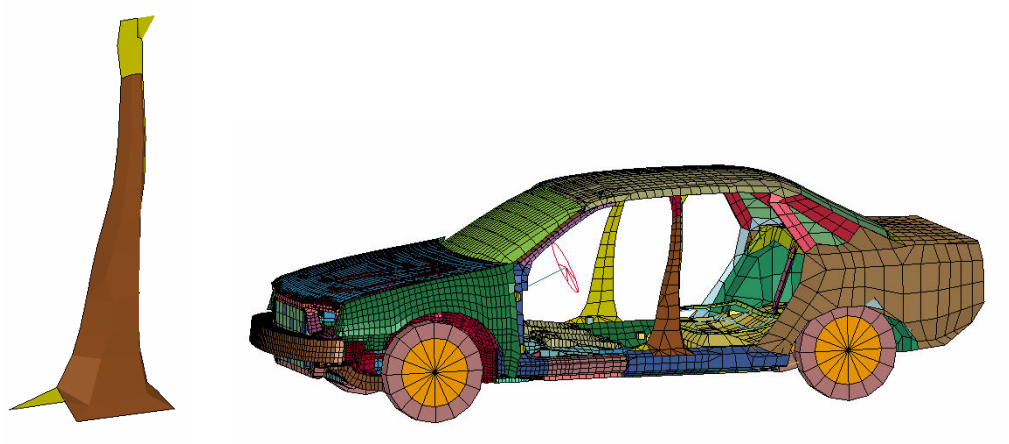

Figure 8. Position of B-Pillar in a car

For the structural analysis of the B-Pillar, Finite Element Method was used since it is the most widely used computational method in the automotive industry.

Steel is still used as the material for this component. However, lighter materials such as the Fiber Reinforced Plastics (FRP) are initiated in the automotive industry. FRP can be used as a substitute for steel for this component as they offer higher energy absorption than the steel. As discussed earlier Composites have high strength and stiffness-to-weight ratio in the fiber direction and as well as the in the direction perpendicular to the fiber even though their Young's Modulus is lesser than the steel. This means that the composites have an increased thickness than the steel and larger second moment of inertia to reduce the effect of elastic bending. There are also some disadvantages of composites, which includes higher production and tooling costs, whereas processing of the complex parts in one piece is much easier. Also, by using composites as the materials for the B-Pillar, reduction in weight can be observed which lead to lesser fuel consumption.

CHAPTER 2

OBJECTIVE AND METHODOLOGY

2.1 Objective

In this study, the objective is to model and analyze a composite B-Pillar instead of the present steel pillar and thus reducing the injuries sustained by the occupant. Efforts are made to reduce the weight of the car without sacrificing the safety of the occupant. As per the crashworthiness standards, which require minimal displacement and higher energy absorption, the use of composite in the safety B-Pillar is proposed and the efficacy of the B-Pillar designed is studied.

There are several areas in the field of crash-impact dynamics that need to be studied to improve the crashworthy design of the B-Pillar. To date, there have been many contributions in understanding and analysis of the energy absorption characteristics. In this study, Finite Element Method is used as an alternative method in studying the energy absorption of a B-Pillar. In addition, one can try to physically understand the behavior by conducting full-scale crash simulations. This is the best possible method, but this is again a very expensive method and can provide information for only a few limited impact conditions and design.

2.2 Methodology

In a crash condition, bending load and progressive crushing absorb most of the crash- related kinetic energy. Structures have to be designed such that they perform the dual role of reacting to both bending loads and progressive crushing in a crash. An attempt is made in this study to composite model a B-Pillar would reduce the injuries sustained by the occupant.

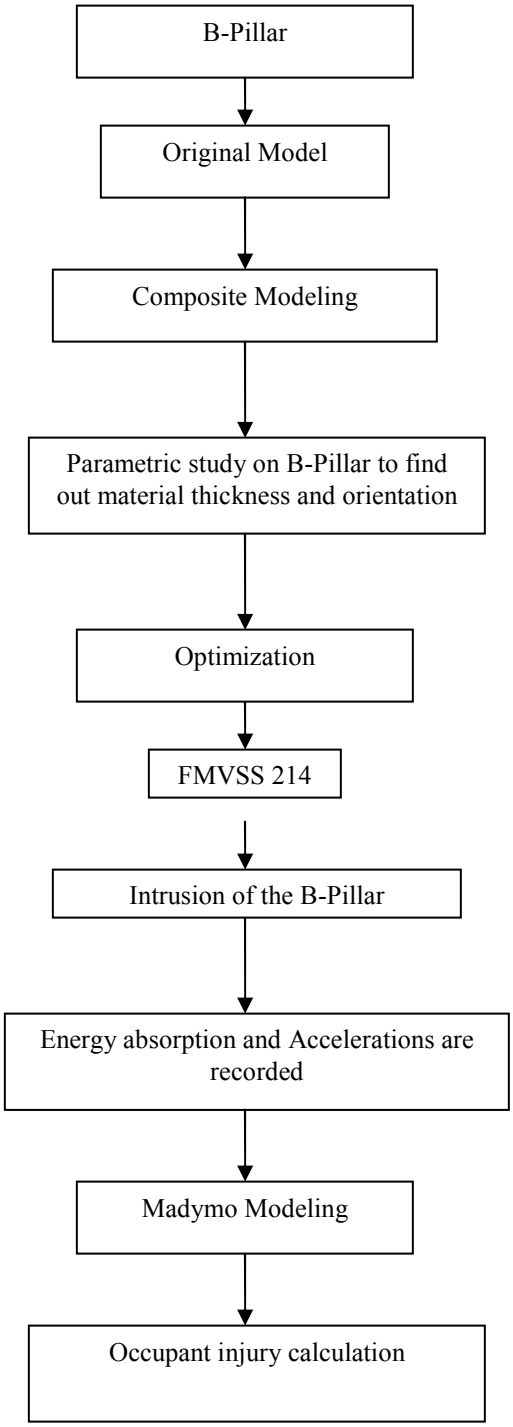

Figure 9. Methodology

Lately, due to the merits of convenience in fabrication, crushing stability and high energy absorbing capability, fiber reinforced composites and their tubular structures have been widely used in vehicles and aircraft.

From figure 9 methodology carried out in this research is depicted.

- This study starts with the composite modeling of car B-pillar where in the B-Pillar is totally made of composite which had proved out to be very efficient.
- Parametric study is carried out on the B-pillar, which included changing the material, layers, orientation and thickness. In order for the B-Pillar to be more energy absorbing these factors are considered.
- Finally, the maximum energy sustained by the B-pillar with the pertinent material, layers orientation and thickness is used for composite modeling. The maximum energy is found out as for the safety of the occupant.
- Intrusion of the B-Pillar is studied.
- Simulation is carried out according to Federal Motor Vehicle Safety Standards (FMVSS) 214 test specifications. These are the standards used for the side impact in a sedan.
- Energy absorption and Accelerations is note down for all the cases and the best energy absorption material is used.
- A Hybrid III 50^{th} percentile side impact dummy is placed in the car. This dummy model created is merged into the car using Easy Crash Dyna.
- Finally, the acceleration pulse values are input to the Madymo model and Injuries sustained by the dummy were compared.

CHAPTER 3

LITERATURE REVIEW

Over the past, crashworthiness has been a growing realization of importance in virtually every transportation sector. Newer designs are proposed every day to improve the crashworthiness of the structure. There is no end in the field of crashworthiness in reducing the injuries sustained by the occupant [3]. It is preferable to design a vehicle to collapse in a controlled manner, thereby ensuring the safe dissipation of kinetic energy and limiting the seriousness of injuries incurred by the occupants.

Use of composites as discussed earlier has increased dramatically over the last few decades. Fiber-reinforced composite materials are characterized by specific stiffness and strength exceeding that of similar metal structures. The prediction of damage to structures caused by accidental collision – whether to automobiles, offshore installations or simply the packaging around an electrical appliance is a crucial factor in the design. With emphasis on light weight vehicles, the use of composite materials in aerospace and automotive structures has created a need to further understand the energy absorption characteristics of composite materials.

Several studies have demonstrated the ability of composite materials to absorb energy under crashworthy conditions [5]. Car safety, gas emission and weight reduction which are the important needs in the design of a car structure are directly influenced by the efficient design and increased use of composite materials. These materials can absorb more deformation and composite materials have high specific strength and high specific stiffness. Composites are lightweight and the manufacturing can be done at a low cost. They also have very high impact load absorbing and damping properties.

3.1 Energy Absorbed Per Unit Mass.

The energy absorbed per unit mass, or specific energy absorption, E, is defined as the energy absorbed by crushing E, per unit mass of deformed structure. Using the notation of Fig, this can be written as [7]:

$$\mathrm{E}_S = \frac{E}{\rho \delta A_{mat}} = \frac{\int_0^{\delta} F dx}{\rho \delta A_{mat}} \tag{3.1}$$

For the ease of analysis, Eq.3.1 is often estimated using an average collapse load, $\overline{F}$ or an average collapse stress $\overline{\sigma}$. This approximate $\mathrm{E}s$, given in Eq 3.2 is sometimes known as specific sustained crushing stress .

$$\mathrm{E}_S \approx \frac{\overline{F}}{\rho A_{mat}} = \frac{\overline{\sigma}}{\rho} \tag{3.2}$$

Specific energy absorption is an especially useful measure for comparing the energy absorption capabilities of different materials for structures in which weight is an important consideration.

3.2 Energy Absorbed Per Unit Volume.

The energy absorbed per unit volume will be of interest in situations in which the space available for energy absorption deformation zone or device is in some way restricted [7]. It may also be appropriate when mechanisms other than deformation of the parent material contribute significantly to a structure's overall energy absorption capability.

3.3 Energy Absorbed Per Unit Length.

The energy absorbed per unit length, E_L from Eq.3.3 is defined as the energy absorbed per unit of deformation distance. This can be expressed as;

$$E_L = \frac{E}{\delta} \tag{3.3}$$

The energy absorbed per unit length provides a convenient and easily measured way of quantifying the crashworthiness of structures where collapse is restricted to a well defined crumple zone [10]. A relatively straightforward crashworthiness specification such as this allows for the ready verification of structures with appropriate test procedures or finite element simulation.

It can therefore be seen that the choice of the most suitable normalized energy absorption parameter for a given circumstance will depend upon the material and geometry of the crushed structure, as well as particular application under consideration.

3.4 B-Pillar And Side-Impact Beam

B-pillars are one of the most sophisticated parts of the automobile body, because this component has to comply with lot of requirements and specifications. There are 2 parts in the B-Pillar, one is the outer layer and the other is the inner layer. These two layers are made of steel and they are welded together [12]. The distance between the B-Pillar and the occupant is very less in side impact when compared to the frontal impact.

Federal Motor Vehicle Safety Standards (FMVSS) No. 214 establishes the minimum strength required for side doors of passenger cars. The side doors must be able to withstand an initial crush resistance of at least 2,250 pounds after 6 inches of deformation, and intermediate crush resistance of at least 3,500 pounds (without seats installed) or 4,375 pounds (with seats installed) after 12 inches of deformation. A peak crush resistance of two times the weight of the vehicle or 7,000 pounds whichever is less(without seat installed) or 3-1/2 times the weight of the vehicle or 12,000 ponds whichever is less(with seats installed) after 18 inches of deformation [9].

3.5 Composites Materials

3.5.1 Composite in automobile parts

Increasing legal and market demands for safety, the weight of the car body will most likely increase in the future. At the same time, environmental demands will become stronger and lower weight will play an important part in meeting them. In the European Union, the car manufacturers have agreed to an overall 25% increase in fuel efficiency by the year 2005 compared to 1990 [10].

Fuel efficiency of the vehicle directly depends on the weight of the vehicle. The carbon fiber composite body structure is 57% lighter than steel structure of the same size and providing the superior crash protection, improved stiffness and favorable thermal and acoustic properties [15].

Composite materials may find the exciting opportunity in the automotive industry as a means of increasing fuel efficiency. With 75 percent of fuel consumption relating directly to vehicle weight, the automotive industry can expect an impressive 6 to 8 percent improvement in fuel usage with mere 10 percent reduction in vehicle weight. This translates into reduction of around 20 kilogram of carbon dioxide per kilogram of weight reduction over the vehicle's lifetime. [17]

Even structural parts like self-supporting car side doors play a role in contributing to the weight reduction without compromise to the existing requirements and will be a cost competitive challenge for future vehicle components. When compared to the passenger car side doors made out of deep drawn steel-sheets, FRP car side doors offer many potential advantages, better NVH-behavior, low specific weight, higher energy

absorption capabilities, and potential of functional integration combined with low production costs [5] .

For the first time FRP's were introduced to the formula-1 in 1980 by McLaren team. Since then the crashworthiness of the racing cars has improved beyond all recognition. Carbon fiber composite has been used to manufacture the body, which is low weight, high rigidity and provided the high crash safety standards. [2]

The report from the United states and Canada predicted that plastics and composites would be widely used applied to body panels, bumper systems, flexible components, trims, drive shaft and transport parts of cars. In addition, rotors manufactured using RTM (Resin Transfer Moldings) for air compressor or superchargers of cars have been used to substitute for metal rotors which are difficult to machine. [6]

3.5.2 Impact damage response on composite materials

A significant amount of research has focused on investigating the damage, crashworthiness, and behavior of dynamic loading under impact. Impact damage in composites occurs when a foreign object causes through the thickness and/or in-plane fracture in the material. The damaged areas can be investigated visually or by using optical or electron microscopy, ultrasonic C-scanning, and acoustic imaging.

Impact damage in composite plates is associated with these major failure modes: delamination, matrix cracking, and fiber breakage. Matrix cracking and delamination are properties of the resin matrix, whereas the fiber breakage is more responsive to the fiber specifications and characteristics and is usually caused by higher energy impacts. [10]

3.5.2.1 Matrix Cracking

Matrix cracking in an impacted composite is caused by tensile stress and by stress concentrations at the fiber-matrix interface. A higher tensile stress results in a

longer and denser cracking pattern. The total energy absorbed by matrix cracking is equal to the product of the surface energy and the small area produced by the crack. Larger crack areas are normally caused by crack branching, in which case the cracks run in the direction normal to the general direction of fracture. In many cases, the surface area created by such cracks is much larger than the area parallel to the primary cracks, increasing the fracture energy significantly. This, in effect, can increase the toughness of composites or the total energy of damage absorbed during impact. [11]

3.5.2.2 Delamination

Different orientation of the plies can promote delamination of two adjacent plies due to the stiffness mismatch at their interface. The delamination areas are influenced directly by changes in the energy of impact. The cracks, which can initiate delamination, can propagate through the plies and may be arrested as the crack tips reach the fiber–matrix interface in the adjacent plies. [5]

3.5.2.3 Fiber Breakage

Fiber breakage can be a direct result of crack propagation in the direction perpendicular to the fibers. If sustained, the fiber breakage will eventually grow to form a complete separation of the laminate. Reaching the fracture strain limit in a composite component results in fiber breakage. For the same impact energy, higher capacity of fibers to absorb energy results in less fiber breakage and a higher residual tensile strength. Secondary matrix damage, which occurs after initial fiber failure, is also reduced allowing residual compressive strength to increase. [19]

3.5.3 Energy absorption in various composite materials

Composites absorb more energy than steel or aluminum. Steel has higher young's modulus, yet fails to absorb higher energy absorption. In composites, there are different

kinds of fibers having different stiffness. For instance from figure 10, carbon fibers are stronger than glass, yet glass fiber withstand load for a longer time than carbon fibers. The energy absorption capability of the composite materials offers a unique combination of reduced weight and improves crashworthiness of the vehicle structures.

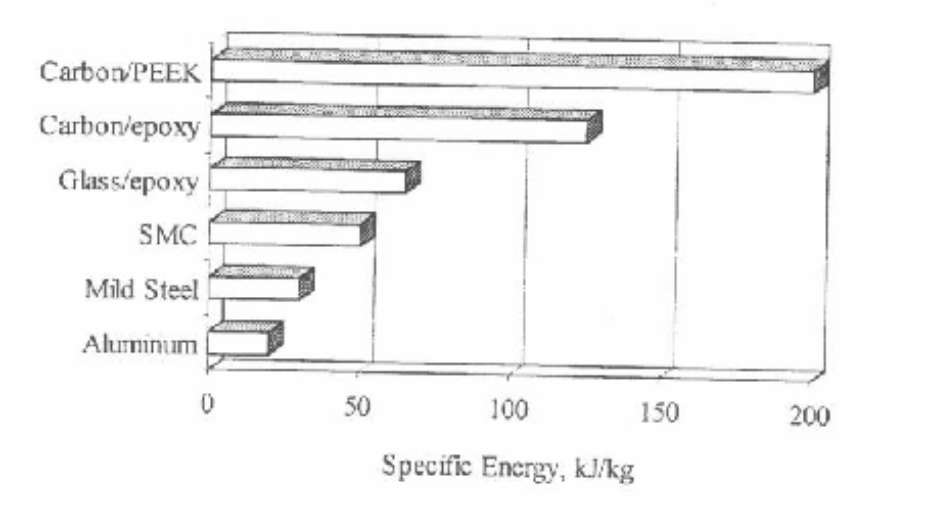

Figure 10. Specific energy of different materials [18]

3.5.4 Properties effecting energy absorption of composite material

In the past, crushing of tube was the method of testing composite specimens and this was primarily used to determine the energy absorption performance of composite materials. [7]

3.5.4.1 Fiber

Farley, reports that, in tests conducted on comparable specimens, carbon fiber reinforced tubes absorb higher energy than those of glass or aramid fibers. This is supported by the data in Table 1 [19]. The reasons for this are related to the physical properties of the fibers, overall failure mechanisms and fiber-matrix bond strengths. [2]

Farley observed that glass and carbon fiber reinforced thermoset tubes progressively crush in fragmentation and splaying modes. Aramid (Kevlar and Dyneema)

fiber reinforced thermo set tubes, on the other hand, crush by a progressive folding mode. Similar results were obtained when impact and static compression tests were carried on Graphite/epoxy, Kevlar/epoxy and Glass/epoxy composite tube specimens respectively. The graphite/epoxy and glass/epoxy angle-ply tubes exhibited brittle failure modes consisting of fiber splitting and ply delamination, whereas the Kevlar/epoxy angle-ply tubes collapsed in a buckling mode. The lower strain to failure of the glass and carbon fibers, which fail at about 1% strain, compared to aramid fibers, which fail at about 8% strain attributes to this difference in behavior. [2]

TABLE 1

SPECIFIC ENERGY ABSORPTION OF DIFFERENT COMPOSITE MATERIALS [19]

Fiber-Matrix	**Lay up**	**Thickness to diameter ratio**	**Specific Energy absorption**
Carbon-Epoxy	$[0/\pm15]_3$	0.033	99
Carbon-Epoxy	$[\pm45]_3$	0.021	50
Aramid-Epoxy	$[\pm45]_8$	0.066	60
Aramid-Epoxy	$[0/\pm15]_2$	0.02	9
Glass-Epoxy	$[0/\pm75]_2$	0.069	53
Glass-Epoxy	$[0/\pm15]_2$	0.06	30
1015 Steel		0.06	42
6061 Al		0.06	44

Results of static crushing tests of graphite reinforced composite tubes were conducted to study the effects of fiber and matrix strain failure on energy absorption helped in drawing the following conclusion: ‘‘To obtain the maximum energy absorption from a particular fiber, the matrix material in the composite must have a greater strain at

failure than the fiber''. The graphite/epoxy tubes had specific energy absorption values greater than that of Kevlar/epoxy and glass/epoxy tubes having similar ply constructions. This is attributed to the lower density of carbon fibers compared to glass and Kevlar fibers. [19]

Research was done on PEEK matrix composite tubes reinforced with AS4 carbon fiber, IM7 carbon fiber and S2 glass fiber respectively. The tubes crushed progressively by the splaying mode. The S2/PEEK tubes displayed approximately 20% lower E_S than the AS4/PEEK and IM7/PEEK tubes though the mean crush stress of S2/PEEK tubes is comparable to that of AS4/PEEK and IM7/PEEK tubes. This is a direct result of the lower density of carbon fiber reinforced materials than the glass reinforced material, since the specific energy absorption is defined as the ratio of the mean crush stress and density of the composite.

A finite element analysis was carried out to model the crushing process of continuous-fiber-reinforced tubes by Farley et al. The analysis is compared with experiments on graphite/epoxy and Kevlar/epoxy tubes. The method obtained a reasonable agreement between the analysis and the experiment. Thornton et al. examined the energy absorption capability in graphite/epoxy, Kevlar/epoxy and glass/epoxy composite tubes. The composite tubes collapsed by fracture and folding mechanisms. The load–compression curves for the graphite/epoxy and the glass/epoxy tubes had similar characteristics but the Kevlar/epoxy composite tubes collapsed by buckling. [8]

In addition, it can be observed from Table 2 [10] that the carbon fibers have high specific energy absorption because of the low density and high strength of the constituent carbon fibers. If aramid fibers are considered, these have low specific energy absorption

than those of carbon. This is because of the reason that the compressive strength of aramid fiber composites is around 20% of the tensile strength. In addition, due to ductile nature, aramid fibers undergo progressive folding failure mechanism. This absorbs energy less efficiently than brittle fracture.

Furthermore, it was possible to optimize the fiber-matrix bond strength of carbon fiber composites through treatment of the fiber's surface. However, in case of aramid and glass fibers it is not possible for such optimization.

TABLE 2

PHYSICAL PROPERTIES OF DIFFERENT FIBERS TYPES [10]

Fiber	**Density (kg/m^3)**	**Axial Young's Modulus (GN/m^3)**	**Tensile Strength (MN/m^3)**
Carbon Fiber (High Modulus)	1950	380	2400
Carbon Fiber (High Strength)	1750	230	3400
Aramid Fiber	1450	130	3000
Glass Fiber	2560	76	2000

3.5.4.2 Matrix Material

The following points can be worth noted about the matrix.

- $G_{1C,}$ higher interlaminar facture toughness, of the thermoplastic matrix material causes an increase in the energy absorption of the composite.
- Increase in the matrix failure strain results in higher energy absorption in brittle fiber reinforcements
- Change in stiffness has very little effect on the energy absorption.

Thornton & Jeryan report that specific energy absorption is a linear function of the tensile strength and tensile modulus of the matrix resin, and that it increases with the

order phenolic < polyester < epoxy for glass fiber tubes. While this observation may be reasonable, it is not conclusively verified by direct reference to material property data (Table 2) because of the spread in reported values [19].

TABLE 3

MECHANICAL PROPERTIES OF RESIN SYSTEMS [10]

Fiber	**Density (kg/m^3)**	**Young's Modulus (GN/m^2)**	**Tensile Strength (MN/m^2)**
Epoxy	1100-1400	2.1-6.0	35-90
Polyester	1100-1500	1.3-4.5	45-85
Phenolic	1300	4.4	50-60

Carbon fiber reinforced composite tubes with different kinds of thermoplastic matrices were studied. From Table 3 [10] the specific energy of thermoplastic tubes follow the order PAS<PI<PEI< PEEK. In a similar study, energy absorption of carbon/PEI (C/PEI), carbon/polyimide (C/PI), carbon/polyarylsulfore (C/PAS), carbon/PEEK (C/PEEK), were investigated and compared with that of carbon/epoxy and glass/polyester. Carbon/thermoplastic tubes demonstrated superior energy absorbing capabilities (E_S=128–194 kJ/kg) than carbon/epoxy (E_S=110 kJ/kg) or glass/polyester (E_S=80 kJ/kg) structures. [10]

3.5.4.3 Fiber & Matrix Combination

The studies described above tend to relate the energy absorption capability of an FRP to the individual properties of its constituent fibers and matrix. It was proposed that energy absorption is substantially dependent on the relative (rather than the absolute) properties of the fibers and matrix. In particular, he reports that the relative values of fiber and matrix failure strain significantly affect energy absorption. It is suggested that to

achieve maximum energy absorption from an FRP, a matrix material with a higher failure strain than the fiber reinforcement should be used. This ensures crushing by high-energy fragmentation. [18]

3.5.4.4 Effect of orientation and lay-up

The orientation of the fibers in a given layer, and the relative orientation of successive layers within a laminate, can significantly affect a component's mechanical properties.

Energy absorption capability varies with ply orientation. Variations in specific energy absorption were observed in tests on $[0/\pm\theta]_3$ carbon/epoxy tubes for $15^o<\theta<45^o$ (Figure 10). Specific energy absorption fell quite markedly over this range. This would suggest that carbon fibers absorb most energy when their orientation tends towards that of the loading. However, it was noted that a laminate consisting entirely of 0^o fibers would be unlikely to have good energy absorption characteristics. In particular, the absence of an outer hoop (90^o) layer can lead to very low energy absorption.

In pertinent to aramid/epoxy it was observed that smaller variations in energy absorption capability for $[0/\pm\theta]_3$ (Figure 10). Specific energy absorption generally increased with increasing θ over the range $45^o<\theta<90^o$. No significant variation was observed for $15^o<\theta<45^o$. This trend is opposite to that observed for carbon-epoxy. [18]

3.5.4.5 Effect of Geometry

These points are some important findings:

- Crush zone mechanisms determine the overall energy absorption of a composite material and

- Specific energy absorption follows the order: circular > square > rectangle for a given fiber lay up and tube geometry.

Thornton and Edwards conducted a study investigating the geometrical effects in energy absorption of circular, square, and rectangular cross section tubes. They concluded that for a given fiber lay up and tube geometry, the specific energy follow the order, circular>square>rectangle.The structural integrity and damage tolerance of typical composite constructed from glass fiber reinforced plastic plays an important role. The effect of the geometry and the strain distribution was investigated using finite element analysis. The results, showed that the critical strains were significantly affected by the joint geometry. This showed that particular defects led to large changes in the strains in the structure [7].

Farley investigated the geometrical scalability of graphite/epoxy and Kevlar/epoxy $[\pm 45]_N$ by quasi-statically crush testing them. All circular cross section graphite/epoxy exhibited a progressive brittle fracturing mode. All Kevlar/epoxy when crushed exhibited the characteristic local buckling crushing mode. It was found that carbon/epoxy exhibited large changes in their energy absorption characteristics with a range of values of diameter (D), wall thickness (t) and (D/t) ratio. In this study, (D/t) ratio was determined to significantly affect the energy absorption capability of the composite materials. [7]

CHAPTER 4

COMPUTER AIDED ENGINEERING TOOLS

Due to increasing cost on conducting real-time crash simulations, CAE tools are very widely used in auto industry. As a result, automakers have reduced product development cost and time while improving safety, comfort, and durability of the vehicles they produce. The predictive capability of CAE tools has progressed to the point where much of the design verification is now done using computer simulations rather than physical prototype testing. Tools used in this study are briefly explained below.

4.1 MSC PATRAN

MSC Patran is one of the versatile software's that deals with design and finite-element analysis. It is a finite element modeler used to perform a variety of CAD/CAE tasks including modeling, meshing, and post processing for FEM solvers LSDYNA, NASTRAN, ABAQUS Etc. Patran provides direct access to geometry from the worlds leading CAD systems and standards. Using sophisticated geometry access tools Patran addresses, many of the traditional barriers to shared geometry, including topological incompatibilities, solid body healing, mixed tolerances, and others.

MSC.Patran provides an open, integrated, CAE environment for multi disciplinary design analysis. This feature can be used to simulate product performance and manufacturing process early in the design-to-manufacture process. This has the ability to import geometry from any CAD system and various data exchange standards.

Powerful and flexible meshing is available with the capabilities that range from fully automatic solid meshing to detailed node and element editing. Loads and boundary conditions can vary and may be associated with the design geometry or with the analysis

model. The result visualization tools enable to identify critical information, including minimums, maximums, trends, and correlations. Isosurfaces and other advanced visualization tools help to speed and improve results evaluation.

In this study, MSC Patran has been used to model the Composite tube. The mesh needed for FEA is generated by this software. The major part of this study, which involves designing of the side-impact beam, is again designed and meshed using MSC Patran. This serves as a very helpful tool in modeling the composites.

4.2 LS-Dyna

LS-DYNA is a general-purpose, explicit finite element program used to analyze the nonlinear dynamic response of three-dimensional inelastic structures. Its fully automated contact analysis capability and error-checking features have enabled users worldwide to solve successfully many complex crash and forming problems [20].

An explicit time integration scheme offers advantages over the implicit methods found in many FEA codes. A solution is advanced without forming a stiffness matrix (thus saving storage requirements). Complex geometries may be simulated with many elements that undergo large deformations. For a given time step, an explicit code requires fewer computations per time step than an implicit one [20]. This advantage is especially dramatic in solid and shell structures. In extensive car crash, airbag and metal forming benchmark analyses, the explicit method has been shown to be faster, more accurate, and more versatile than implicit methods.

LS-DYNA has over one hundred metallic and nonmetallic material models like Elastic, Elastoplastic, Elasto-viscoplastic, Foam models, Linear Viscoelastic, Glass Models, Composites, etc.

The fully automated contact analysis capability in LS-DYNA is easy to use, robust, and validated. It uses constraint and penalty methods to satisfy contact conditions. These techniques have worked extremely well over the past twenty years in numerous applications such as full-car crashworthiness studies, systems/component analyses, and occupant safety analyses. Coupled thermo-mechanical contact can also be handled. Over twenty-five different contact options are available. These options primarily treat contact of deformable to deformable bodies, single surface contact in deformable bodies, and deformable body to rigid body contact. Multiple definitions of contact surfaces are also possible. A special option exists for treating contact between a rigid surface (usually defined as an analytical surface) and a deformable structure. One example is in metal forming, where the punch and die surface geometries can be input as IGES or VDA-surfaces which are assumed rigid. Another example is in occupant modeling, where the rigid-body occupant dummy (made up of geometric surfaces) contacts deformable structures such as airbags and instrument panels [20].

Some of the prime application areas of LS-DYNA are as follows:

- Crashworthiness simulations: automobiles, airplanes, trains, ships, etc.
- Occupant safety analyses: airbag/dummy interaction, seat belts, foam padding.
- Bird strike.
- Metal forming: rolling, extrusion, forging, casting, spinning, ironing, superplastic forming, sheet metal stamping, profile rolling, deep drawing, hydroforming (including very large deformations), and multi-stage processes.
- Biomedical applications and many more.

LS-DYNA runs on leading UNIX workstations, supercomputers, and MPP (massively parallel processing) machines. Computer resource requirements vary depending on problem size. Simulations with more than 1.200.000 elements have been run using 250 million words of memory and 3.5 GB of disk space. On supercomputers, the code is highly vectorized and takes advantage of multiple processors [20].

LS-Dyna is used to simulate the crushing process of a composite tube and it is used to compare the different composite materials in determining the most energy absorbing material. Three point bending test is also carried out using this FEA solver. The side-impact B-Pillar designed is placed in the car and then side-impact analysis is carried in LS-Dyna. Finally, MADYMO/LS-Dyna is coupled to determine the injuries sustained [20].

4.3 MADYMO

MADYMO (MAthematical DYnamical MOdels) is a general-purpose software package, which can be used to simulate the dynamic behavior of mechanical systems [21]. Although originally developed for studying passive safety, MADYMO is now increasingly used for active safety and general biomechanics studies. It is used extensively in industrial engineering, design offices, research laboratories and technical universities. It has a unique combination of fully integrated multibody and finite element techniques.

MADYMO combines in one simulation program the capabilities offered by multibody, for the simulation of the gross motion of systems of bodies connected by complicated kinematical joints and finite element techniques, for the simulation of

structural behavior. It is not necessary to include both in a model, i.e. a model with either finite elements or multibodies can be used [21].

The multibody algorithm in MADYMO yields the second time derivatives of the degrees of freedom in explicit form. The number of computer operations is linear in the number of bodies if all joints have the same number of degrees of freedom. This leads to an efficient algorithm for large systems of bodies. At the start of the integration, the initial state of the systems of bodies has to be specified (initial conditions). Several different kinematic joint types are available with dynamic restraints to account for joint stiffness, damping and friction. Joints can be unlocked or removed based on a user defined criterion.

Planes, ellipsoids, cylinders and facet surfaces can be attached to a body to represent its shape. These surfaces are also used to model contact with other bodies or with finite elements. The contact surfaces are of major importance in the description of the interaction of the occupant with the vehicle interior. The elastic contact forces, including hysteresis, are a function of the penetration of the contact surfaces. In addition to elastic contact forces, damping and friction can be specified.

The output generated by MADYMO is specified through a set of output control parameters. A large number of standard output parameters are available, such as accelerations, forces, torques and kinematics data [21]. MADYMO offers in addition to standard output quantities, the possibility to calculate injury parameters like femur and tibia loads, Head Injury Criterion (HIC), Gadd Severity Index (GSI), Thoracic Trauma Index (TTI) and Viscous Injury Response (VC). Special output can be obtained through

user-defined output routines. Results of the simulation are stored in a number of output files, which are accessible by post-processing programs.

4.4 EASI CRASH DYNA (ECD)

EASI CRASH DYNA is the first fully integrated simulation environment specially designed for crash engineering requiring large manipulation capability [20]. It can directly read files in IGES, NASTRAN, PAM-CRASH, MADYMO and LSDYNA data. ECD has unique features, which enable the crash simulation more realistic and more accurate. These are

4.4.1 Pre-Processing Features

- Fully automatic meshing and automatic weld creation.
- Rapid graphical assembly of system models.
- FE-Dummy and Rigid body dummy structuring, positioning and orientation.
- Material database access and manipulation.
- Graphical creation, modification and deletion of contacts, materials, constraints and I/O controls.
- Automatic detection and correction of initial penetration.
- Replacing the component from one model to another model.

4.4.2 Post-Processing Features

- Highly optimized loading and animation of DYNA results for design.
- Superposition of results for design.
- User friendly and complete plotting for processing simulation and test data comparisons.
- Quick access to stress energies and displacements without reloading the file.

- Dynamic inclusion/exclusion of parts during animation and visualization.
- Import and super-imposition of test results with simulation results.
- Synchronization between animation and plots, between simulation result file and test result file.

4.5 Easi-Crash Mad

EASi-CRASH is based on EASi's 10 years of practical experience in crash simulations. It greatly enhances the simulation process by allowing concurrent access to the model and simulation results. Animation, visualization and synchronized curve plotting make EASi-CRASH MAD a high performance CAE environment [21]. The preprocessing features are listed below.

- Graphical creation, modification and deletion of multi-bodies and FE entities.
- FE meshing and manipulation capabilities.
- Graphical display, browsing and editing of MADYMO entities through browser interface (MADYMO explorer).
- Supports INCLUDE files.
- Card Image representation of MADYMO input deck.
- Quick JOINT definition and orientation.
- Easy dummy positioning .
- Rapid contact creation, modification and preview through Contact spreadsheet.
- High speed generation of MADYMO and FE seat belt using automated belt routing techniques.
- Supports advanced airbag modeling (CFD).

CHAPTER 5

SECTION MODEL AND ANALYSIS OF B-PILLAR IMPACT WITH SPHERE

5.1 Design of B-Pillar

B-pillars are one of the most sophisticated parts of the automobile body, because this component has to comply with lot of requirements and specifications. The distance between the B-Pillar and the occupant is very less in side impact when compared to the frontal impact. In addition, when the impact occurs, the B-Pillar or structures in the B-Pillar have to absorb more energy with minimal acceleration to the occupant. [12]

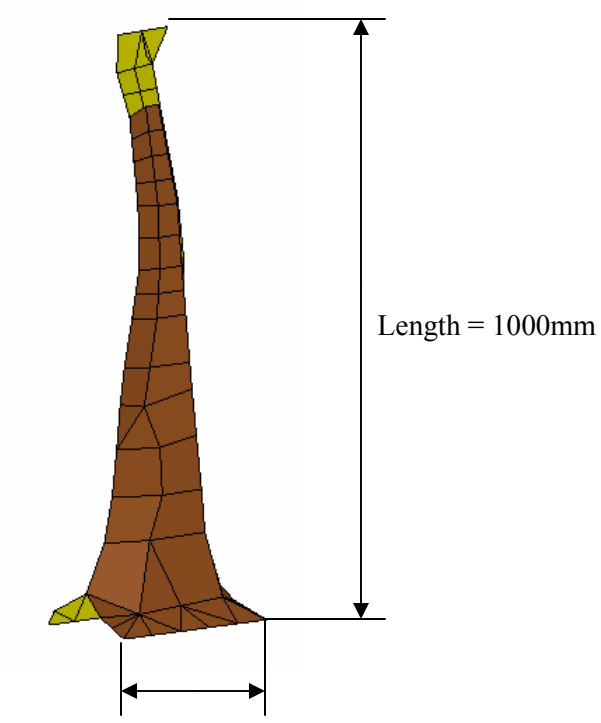

Figure 11. B-Pillar

The new design as in figure 11 is intended to develop and demonstrate the use of carbon fiber composite structures to generate significant weight savings for an automobile. The first phase was a structural design study. This study proposed variable thickness panels to maximize the structural efficiency at minimum mass. The wall thickness is constrained to be at 3.9mm.

For the structural analysis of the B-Pillar, Finite Element Method was used since it is the most widely used computational method in the automotive industry.

Steel is still used as the material for this component. However, lighter materials such as the Fiber Reinforced Plastics (FRP) are initiated in the automotive industry. FRP can be used as a substitute for steel for this component as they offer higher energy absorption than the steel. As discussed earlier Composites have high strength and stiffness-to-weight ratio in the fiber direction and as well as the in the direction perpendicular to the fiber even though their Young's Modulus is lesser than the steel. This means that the composites have an increased thickness than the steel and larger second moment of inertia to reduce the effect of elastic bending. There are also some disadvantages of composites, which includes higher production and tooling costs, whereas processing of the complex parts in one piece is much easier. Also, by using composites as the materials for the B-Pillar, reduction in weight can be observed which lead to lesser fuel consumption.

Figure 11 gives a basic description of the B-Pillar with composite as the material. In this model shell elements are used with the number of integration points being 13. The orientation that is use used for the composite is (0,30,-30,60,-60,90,0,90,-60,60,-30,30,0). The number of nodes and elements present are shown in Table 4. The weight of the

composite B-Pillar is reduced drastically when compared to the present B-Pillar. The weight of the composite B-Pillar is 1.04 kg where as the weight of the present B-Pillar made of steel is 2.15 kg. The weight of the composite is 53% less when compared to the steel B-Pillar. This shows the weight reduction when a composite material is used.

TABLE 4

PROPERTIES OF B-PILLAR

Number of Nodes Number of	433
Number of Elements	754
Material	Carbon fiber
Thickness	3.9mm
Weight	1.05kgs

5.2 Impactor

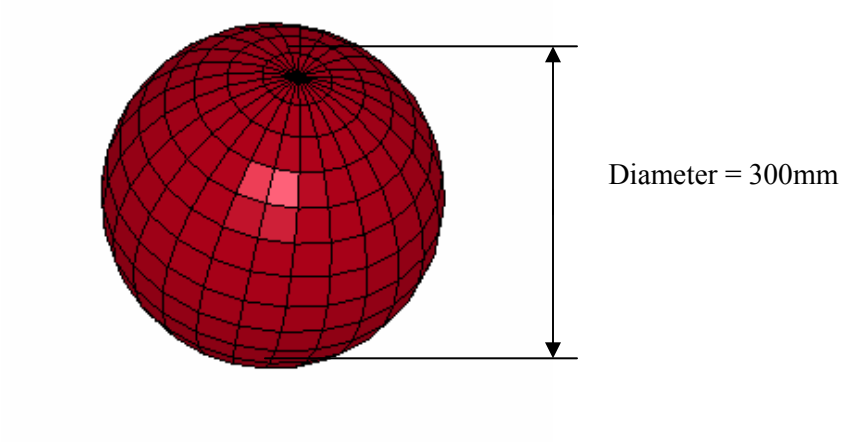

Figure 12. Sphere (Impactor)

Figure 12 shows the impactor. The geometry of the impactor is chosen as a sphere. The impactor is made of honeycomb material whose behavior is anisotropic and is a solid. This material is chosen since the barrier in FMVSS 214 regulation is of the same material. Table 5 shows the properties with the number of nodes and elements [7]. Thornton and Edwards conducted a study investigating the geometrical effects in energy absorption of circular, square, and rectangular cross section tubes. They concluded that for a given fiber lay up and geometry, the specific energy follow the order, circular>square>rectangle.

TABLE 5

PROPERTIES OF SPHERE

Number of Nodes Number of	1616
Number of Elements	1600
Material	Honeycomb
Weight	5.12kgs

5.3 Analysis of B-Pillar impact with sphere

B-pillars are one of the most sophisticated parts of the automobile body, because this component has to comply with lot of requirements and specifications. The distance between the B-Pillar and the occupant is very less in side impact when compared to the frontal impact. In addition, when the impact occurs, the B-Pillar or structures in the B-Pillar have to absorb more energy with minimal acceleration to the occupant.

Therefore this simulation is carried out as verification for FMVSS 214 regulations and to show that composite B-Pillar can be used for the actual side impact.

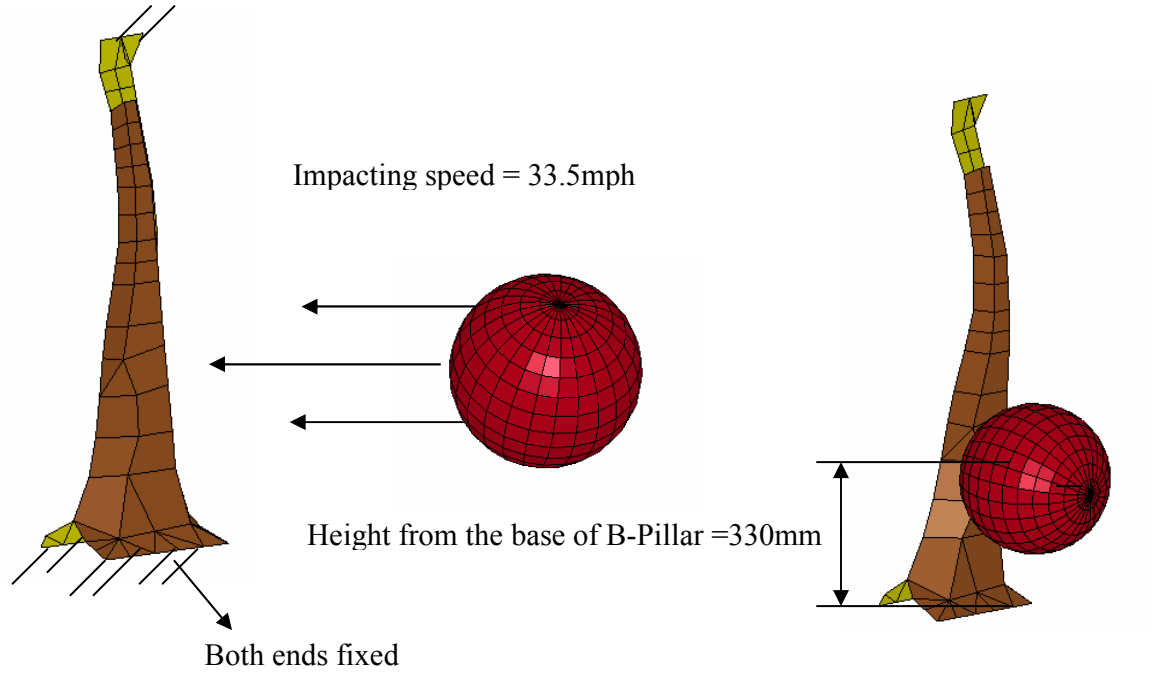

Figure 13. B-Pillar section model with sphere

Figure 13 shows the model of a B-Pillar of a car with an impact object, the sphere. The sphere is made of honeycomb material with diameter 300mm. Honeycomb material is used because this is the actual material that is used in the moving deformable barrier according to federal motor vehicle standards. The impactor is at a height of 330mm from the base of the B-Pillar. The top and the bottom nodes of the B-Pillar are constrained in all directions. Initial velocity is given on the sphere which is 33.5mph.The analysis is run for 0.012 seconds and then the results are noted. The elements used in the B-pillar are shell elements that are elastic plastic elements. The point of contact of the impactor is same as the contact of the barrier according to the regulations [9]. Three different materials are used for the B-Pillar which are steel, glass and carbon fiber.

Results are compared and the best material is used in the B-Pillar. In this case carbon proved out to be the best material as the energy absorption of carbon is twice as that of steel which is the original material. Figure 14 shows the fringe levels at different times.

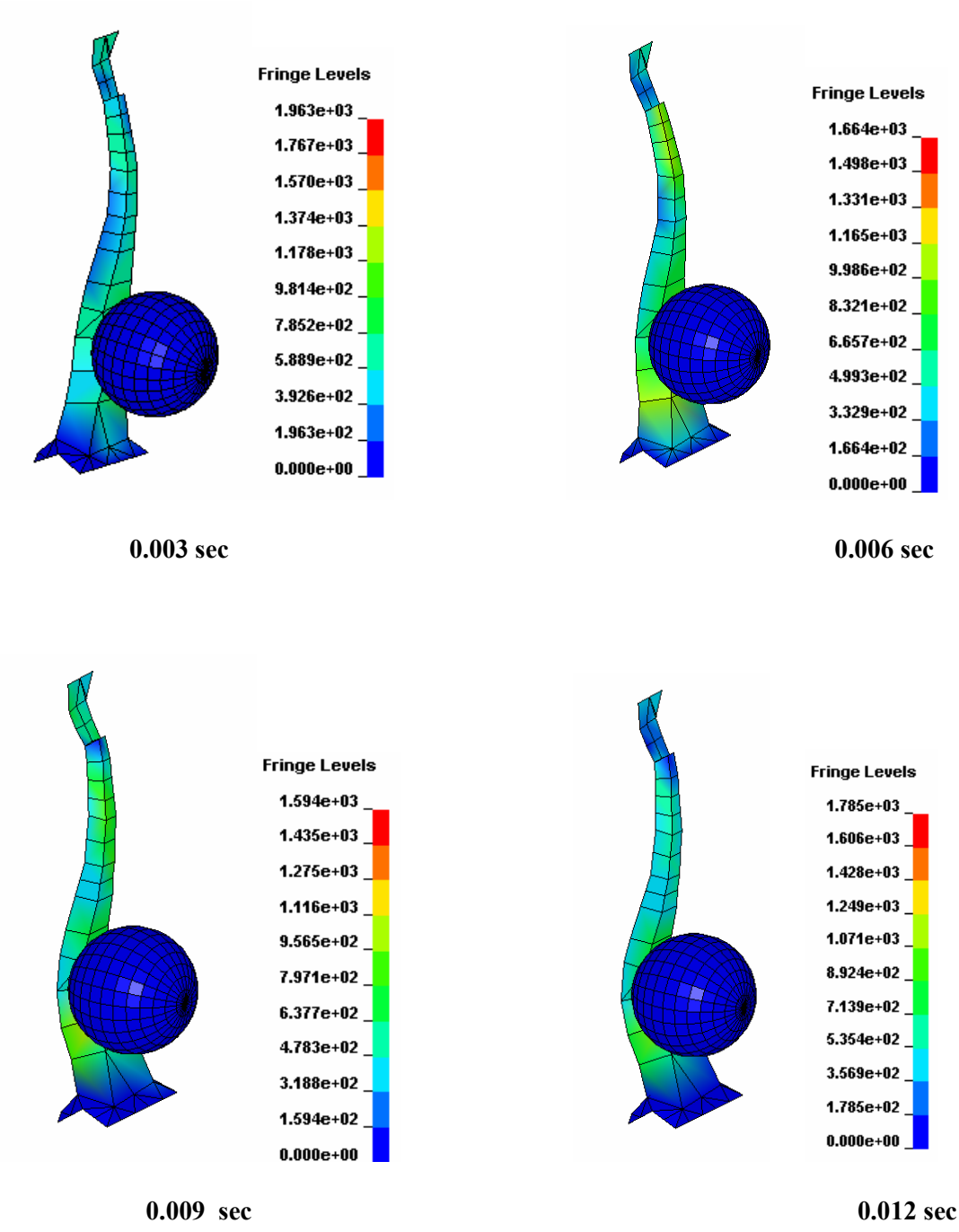

Figure 14. Fringe levels for B-Pillar

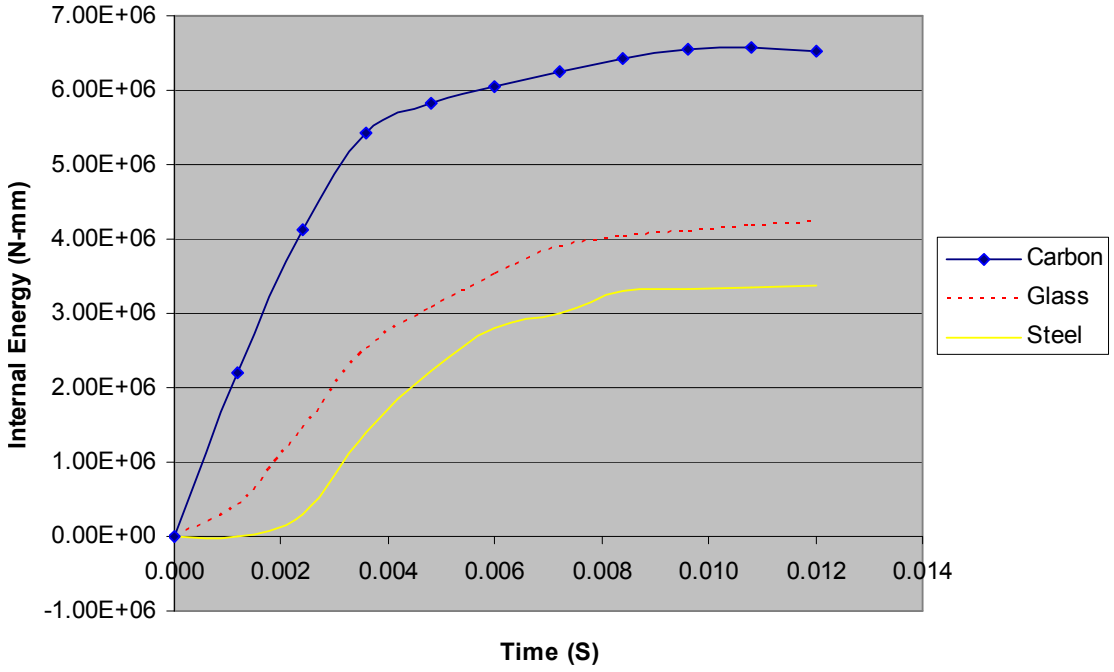

Figure 15. Internal Energy v/s Time for different materials

TABLE 6

SPECIFIC ENERGY ABSORPTION OF DIFFERENT MATERIALS

Material	Energy Absorption
Carbon Fiber	6.52e+6 N-mm
Glass fiber epoxy	4.24e+6 N-mm
Steel	3.58 e+6 N-mm

Table 6 shows energy absorbed by different materials. Carbon fiber absorbs almost twice the energy when compared to steel. The thickness of carbon fiber is 3.9mm and is made of shell elements. Figure 15 shows time vs. internal energy graph. Internal energy of the material specifies the ability of the material to withstand the load while it is deformed. Higher the internal energy, higher will be ability of the material in taking the load and therefore the energy absorption of the material increases. From figure 15 the end

time specific energy absorption of carbon is very high when compared to steel and glass. Thus, it can be concluded that carbon fiber with thickness at 3.9 mm has higher energy absorption. Therefore, these are the parameters considered when analyzing the B-Pillar.

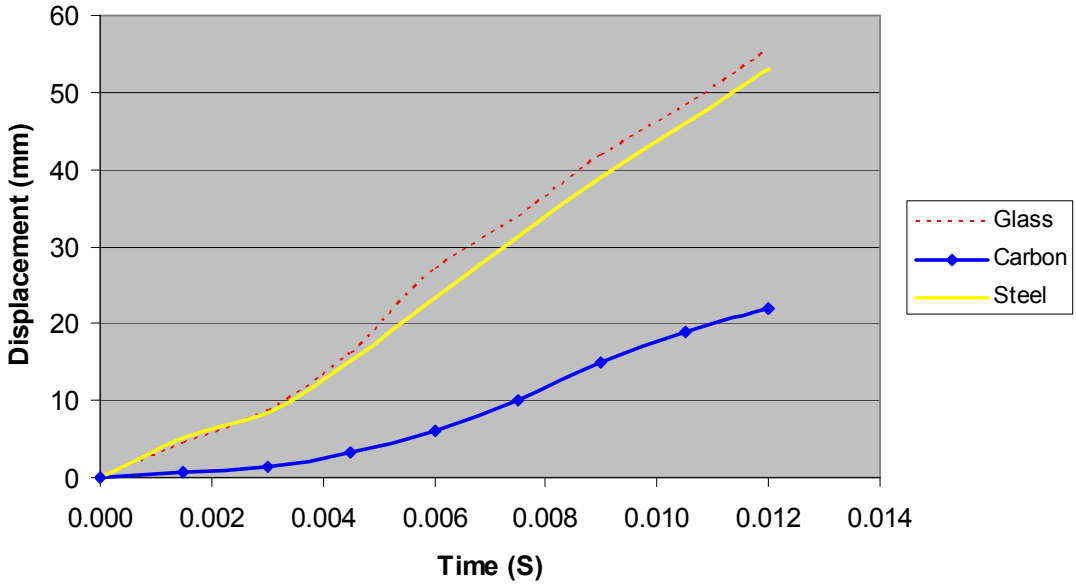

Figure 16. Displacement of the B-Pillar

5.4 Displacements of the B-Pillar

Figure 16 shows the Displacements of the B-Pillar in pertinent to time. Different materials such as steel, Glass fiber and Carbon fiber are illustrated. The curve is self-explanatory with the Glass fiber and steel having almost no difference in the displacement. Since the density of glass is very high compared to carbon fiber the ability for glass to withstand load is very less. However, B-Pillar with carbon fiber shows very less displacement. This indicates that there is very less intrusion into the occupant cabin, which results in reducing the fatal injuries caused by side impact. Area under the curve for carbon shows the amount of intrusion in the car.

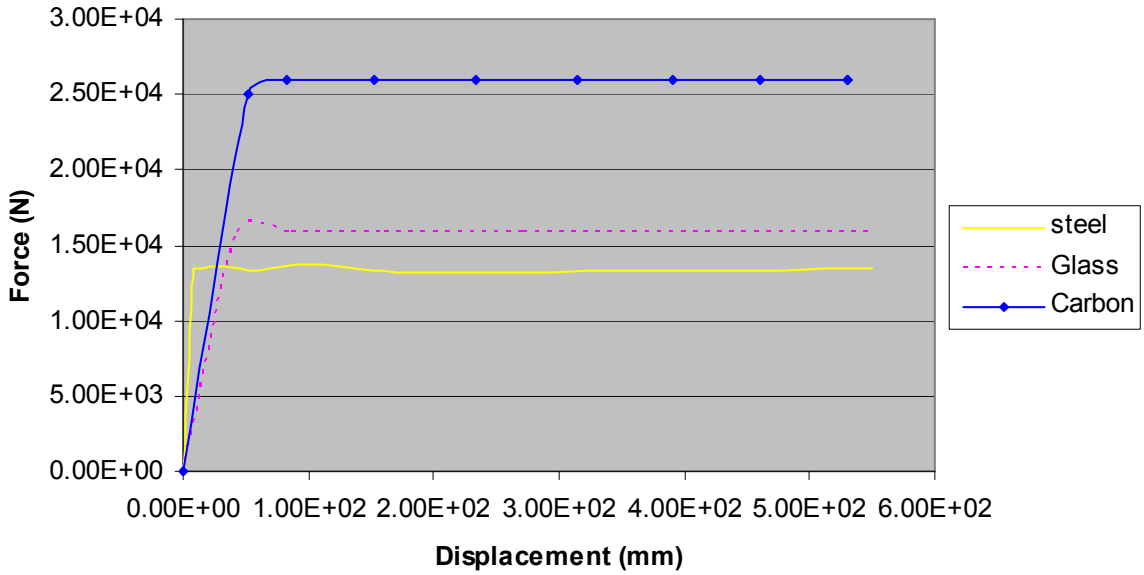

Figure 17. Force v/s Displacement for different materials

Force v/s Displacement for different materials such as steel, Glass fiber and Carbon fiber are illustrated. As the area under the curve indicates the energy absorbed by the structure, it is evident from figure 17 that the structure with carbon fiber material absorbs more energy. The carbon fiber as seen has a higher ability to withstand load. This means that the injury sustained by the occupant in a vehicle is reduced considerably. This is the reason why carbon fiber can be used in the B-Pillar.

The least energy absorbing material is steel as per the study. This means that the injury sustained by using steel is more when compared to carbon. Glass fiber also gives the same properties as steel as the density of glass is more than carbon. Hence, it is not advisable to use either steel or glass fiber as the material for the B-Pillar. However, the initial peak loads of carbon fiber is high and this might induce more forces on the occupant. However, the high sustaining load offered by the carbon fiber, which absorbs higher energy thus reducing the injuries, fixes this issue.

CHAPTER 6

SIDE IMPACT MODELING AND ANALYSIS OF B-PILLAR IN A SEDAN

Federal Motor Vehicle Safety Standard (FMVSS) 214 is the standard used for side-impact crash analysis [9]. This was developed by NHTSA (National Highway Traffic Safety Administration) [28]. In this, a deformable barrier (MDB) is made to strike a stationary car according to federal motor vehicle safety standards. A side impact dummy is placed in the driver's side of the car to record the injuries. Ford Taurus is the standard car used in the side-impact crash analysis and this model is explained in detail in the next section.

6.1 Finite element study of Ford Taurus

Due to the increasing cost of conducting an experiment, finite element models are used everywhere. Automotive industry is the filed, which utilizes the FEM to the most. Finite Element Models are accurate to simulate several different crash tests and predict the vehicle and occupant response various crash scenarios. Such a design leads to minimize the time and the cost of the testing process and helps in making effective safety decisions.

The Ford Taurus model used for the analysis is a four-door sedan with 5 meters length and 2.76 m wheelbase. It is developed by NHTSA. Figure 18 shows the finite element model of Ford Taurus Model. It has 134 parts, which represent different vehicle parts and these parts are joined by rigid body constrained options and spot-weld. The contacts between different parts are modeled as single surface sliding interface (AUTOMATIC_SINGLE_SURFACE).

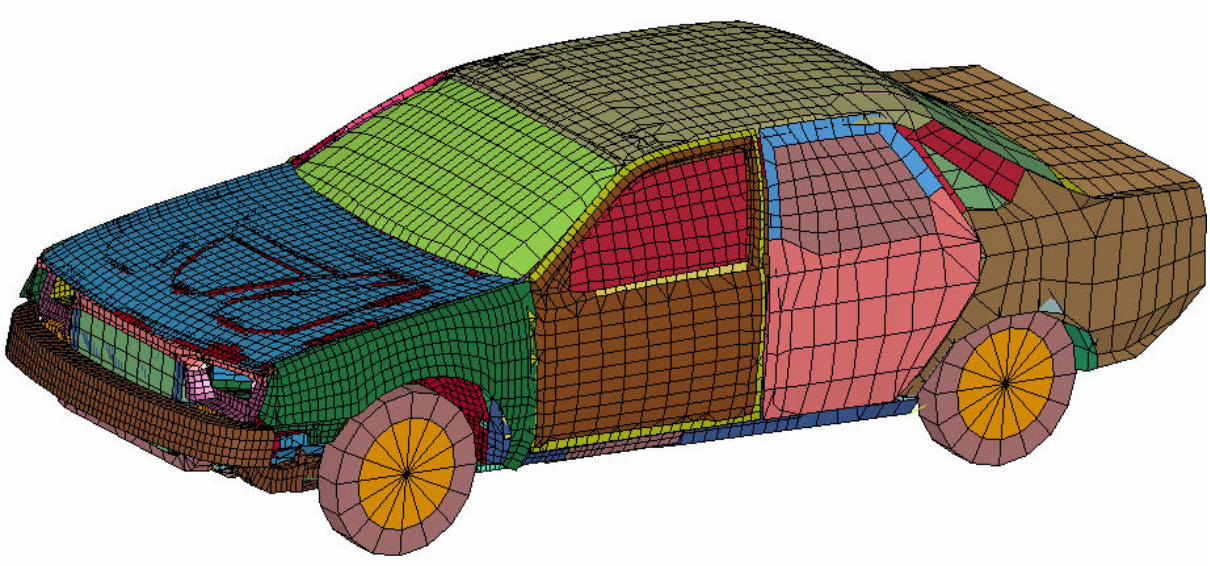

Figure 18. Ford Taurus model [28]

TABLE 7

FINITE ELEMENT SUMMARY OF FORD TAURUS [28]

Number of Parts	134
Number of Nodes	26797
Number of Quad Elements	23124
Number of Tria Elements	4750
Number of Hexa Elements	338
Number of Penta Elements	10

Table 7 depicts the finite element summary of Ford Taurus. It consists of 134 parts and these represent the different parts of the vehicle. Two different types of shell elements are used, triangular and quadrilateral. This model consists of shell, B-Pillar and the solid elements. The shell elements have isotropic elastic plastic material and eight stress strain points define the stress strain relationship. B-Pillar elements are assigned

with isotropic elastic material and the solid elements have honeycomb material with constant stress element formulation.

6.2 Impactor Modeling

Impactor used in FMVSS 214 is a moving deformable barrier (MDB) which was designed to be representative of the mass and size of U.S. vehicles. The relative longitudinal and lateral speed of the MDB and the target vehicle is considered the threshold for serious injury in actual crashes. The finite element model of the barrier is shown in figure 19.

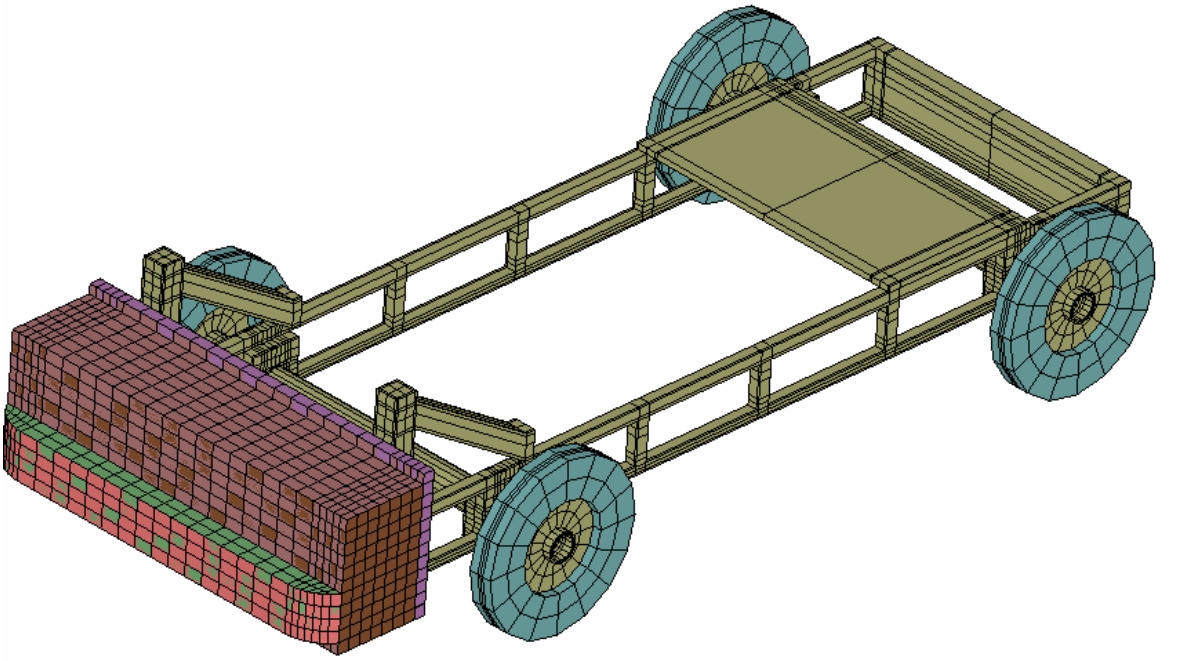

Figure 19. FEM model of MDB [28]

The MDB face assembly includes a bumper constructed of honeycomb 1690+/-103 kPa sandwiched between 3.2 mm thick aluminum plates. The bumper is a flexion member and develops flexion strength based on the material properties of these front and back plates.

The aluminum material for honeycomb structure of the barrier face is specified by design. The bottom edge of the MDB is 279 mm from the ground. The protruding portion of the barrier simulating a bumper is 330 mm from the ground. Figure 20 and 21 shows the specifications of MDB. The MDB has total mass of 1367 Kg. For defining material model in LS-DYNA for honeycomb structure of the barrier face, MAT_HONEYCOMB card has been defined [28]. Summary of the FEM barrier is illustrated in Table 8.

TABLE 8

SUMMARY OF MDB [28]

Number of Parts	8
Number of Nodes	11033
Number of Quad Elements	718
Number of Hexa Elements	7324

The specifications of the MDB are described in detail in figure 21

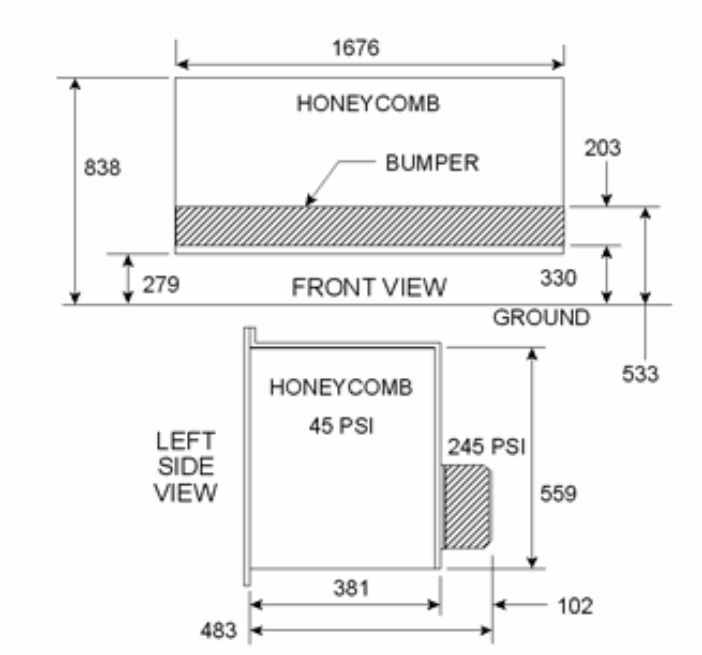

Figure 20. Specifications of MDB [28]

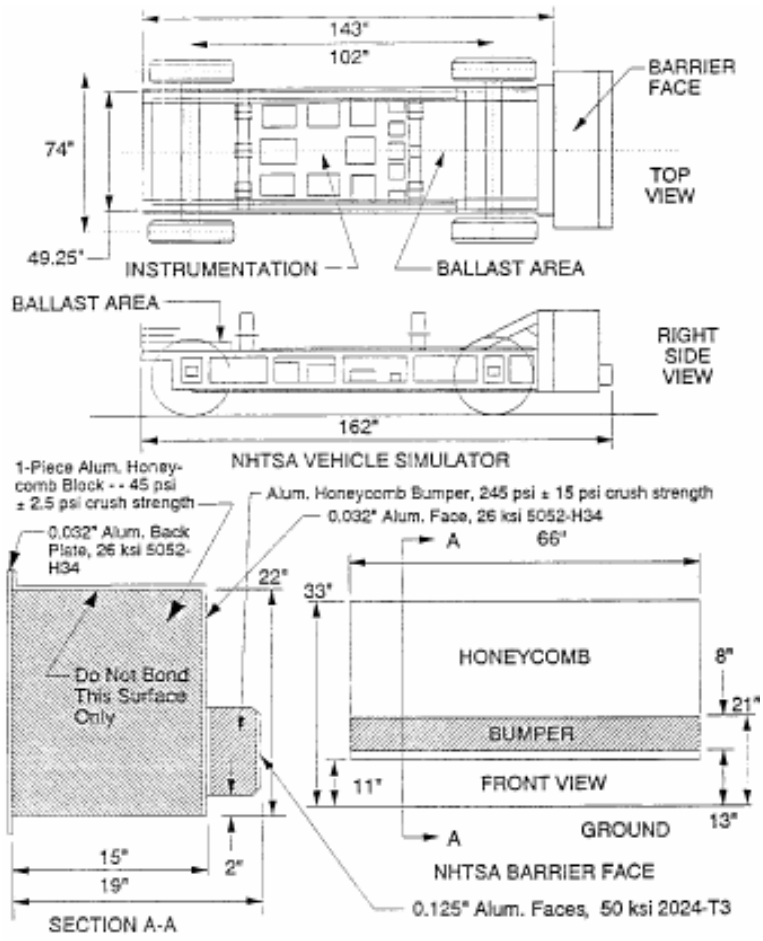

Figure 21. Dimensions of Moving Deformable Barrier (MDB) [28]

6.3 Side-Impact Analysis

6.3.1 LS-Dyna simulation

According to the FMVSS 214 standard, the barrier moves in the direction of the car and strikes the driver side of the car at a crabbed angle of 27° with the velocity of the barrier at 33.5 mph. The distance between the vehicle and the barrier is kept to the minimum in order to minimize the simulation time [9]. This simulation is run for 0.12s and figures 22 shows animation sequence of the side-impact crash analysis.

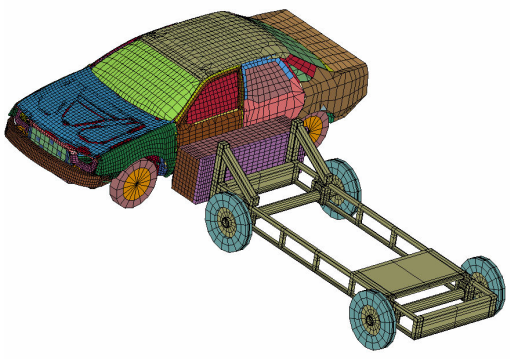

Time = 0 sec

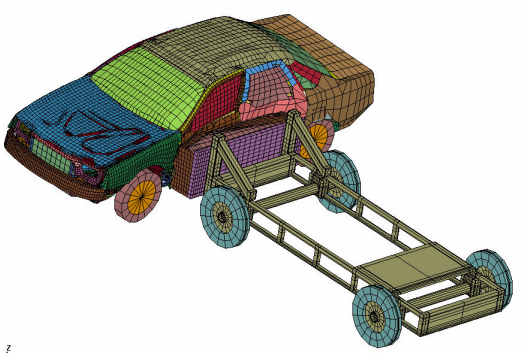

Time = 0.04 sec

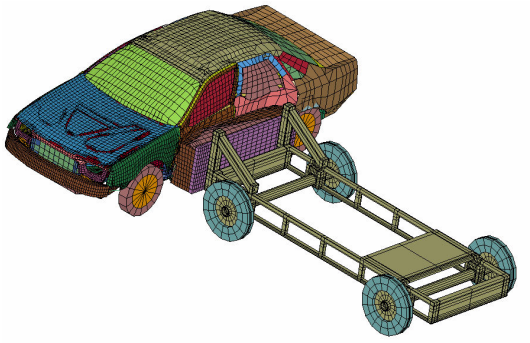

Time = 0.08 sec

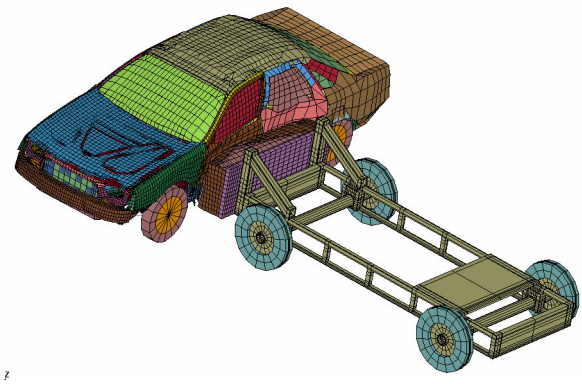

Time = 0.12 sec

Figure 22. Animation sequence of a side-impact crash analysis

According to the figure 22, it can be noticed that there is considerable deformation sustained by the Ford Taurus sedan. The MDB has had almost even damage, but it passes all its energy into the side door of a car. As a reason the side door of the car should have the ability to withstand the load so that there is less injury on the occupant of the vehicle.

6.4 Fiber Orientation

The parametric study on the B-Pillar is carried out by starting with the variation in lay-up sequence. Four different lay-up sequences are analyzed and they are as follows. The material used while altering the lay-ups is glass fiber and carbon fiber.

1) $[(\pm 45°)_6/90°]$
2) 0,30,-30,60,-60,90,0,90,-60,60,-30,30,0
3) 45,-45,45,-45,45,-45,0, 45,-45,45,-45,45,-45
4) 0,45,0,45,0,45,0,45,0,45,0,45,0
5) 0,90,0,90,0,90,45,90,0,90,0,90,0

Finding out an orientation which is more energy absorbing is a complicated issue. Deciding the directions of lay-up for the specimen is very important. These above orientations are commonly used and are compared using the Force v/s Displacement curve and the energy dissipated in each specimen. In addition, the energy absorbed in these specimens are also investigated and compared. Finally, an orientation with a high-energy absorption is chosen for further study in this research. Figure 23 shows the corresponding curves for the above mentioned lay-up sequences. From the graph it can be seen that, area under the curve for the layup sequence 0,30,-30,60,-60,90,0,90,-60,60,-30,30,0 is more and thus energy absorbed is more in this orientation.

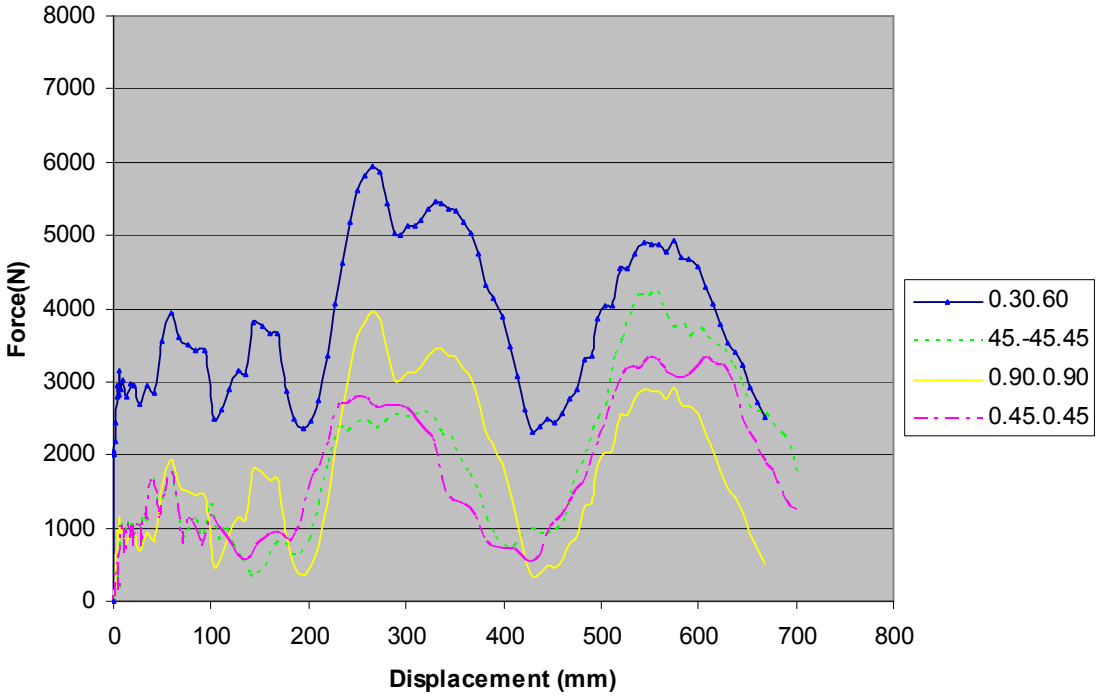

Figure 23. Force v/s Displacement for different orientations

It can also be seen that the load sustained by this orientation is higher than any other orientation. The next higher sustaining load is the (45,-45,45,-45,45,-45,0, 45,-45,45,-45,45,-45). However, the deformation pattern in this orientation is not progressive and this cannot absorb more energy than the #1 orientation. In addition, from the figure 23 it can be seen that the orientation #1 has higher energy than any other orientation. This means that this orientation has the ability to withstand higher load than any other orientation.

Finally, comparing the energy absorption values from figure 23, it can be concluded that the orientation (0,30,-30,60,-60,90,0,90,-60,60,-30,30,0) has better energy absorption and this is used in every composite part designed in this study.

6.5 Thickness

Thickness of the structure plays a vital role in energy absorption of a material. By increasing the thickness, the structure can be made to withstand more load and thus more energy absorption. However, the volume also increases when there is any increase in thickness and this in turn increases the mass of the structure. This not acceptable in the filed of crashworthiness as weight plays a very critical role in increasing the fuel efficiency of the vehicle.

In this study, thickness is varied to 1.3 mm and 3.9 mm. When the 1.3 mm thickness is used, the deformation is very much and the deformation pattern is completely different. In addition, the energy absorption is very less. The 3.9 mm thickness yielded very good energy absorption. Therefore, 3.9mm thickness is used in every composite part

Once the orientation and the thickness are decided, the next step is to find a material that has higher energy absorption. Keeping the orientation to 0,30,-30,60,-60,90,0,90,-60,60,-30,30,0 and thickness at 3.9 mm, different materials are analyzed which included Carbon/Epoxy, Glass-fiber epoxy and Steel. The properties of these materials are shown in Table 11 of Appendix A respectively. Figure 26 shows the Force v/s Displacement of different materials considered.

6.6 Analysis of B-Pillar

The new modelled B-Pillar is placed in the car as shown in figure 24. Easi-Crash Dyna is used to merge the B-Pillar with the car. ECD is also used to assemble the newly designed side-impact B-Pillar. This analysis is done using FMVSS 214 standards. First of all FMVSS 214 standard is used to study the deformation sustained by the car when using the new designed B-Pillar.

It has already been decided earlier in this study that carbon fiber composite is stronger and absorbs more energy. In this chapter, this is proved again by implementing the new-modelled composite B-Pillar in the car. In addition, glass fiber results are also included to help in interpreting the results.

6.6.1 FMVSS 214 test

As discussed earlier, in this test, a MDB is made to impact the side of the car at 33.5 mph. The MDB moves at a crabbed angle of 27° [9].

6.6.2 Simulation of side impact crash with the present B-Pillar

The full Side Impact model is carried out in LS-DYNA for 0.1 seconds. The accelerometers are placed at eight locations (near the driver side) in the vehicle. The contacts are defined by geometric interface. Figure 24 shows the deformation sustained when MDB crashes into the car.

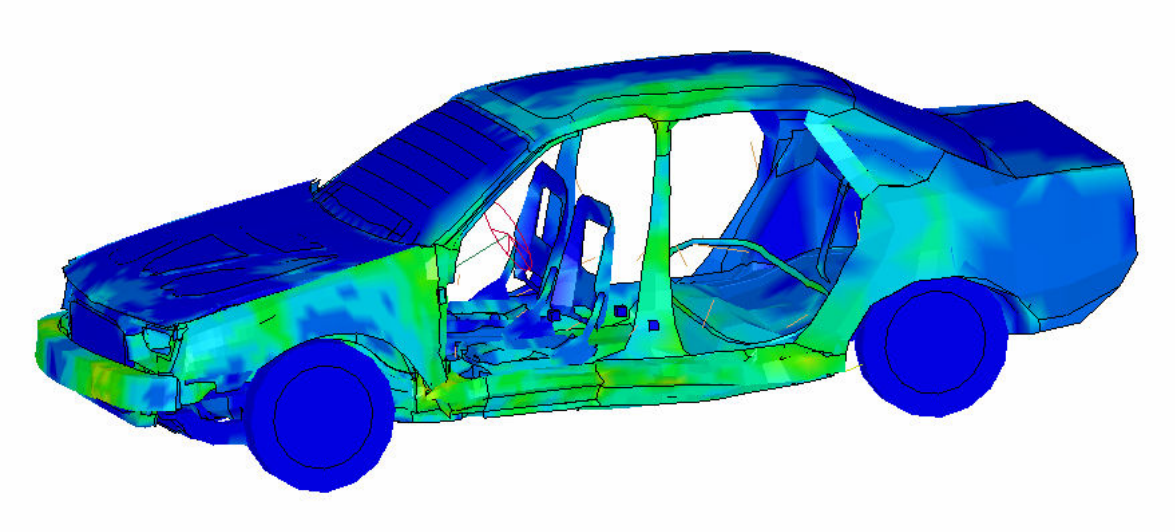

Figure 24. Deformation in the present B-Pillar

6.6.3 Simulation of side impact crash with Composite B-Pillar

The present B-pillar in the Ford Taurus car was removed using ECD and the composite B-Pillar was merged with car. Deformation sustained by the car while using the carbon fiber reinforced composite B-Pillar is shown in figure 25.

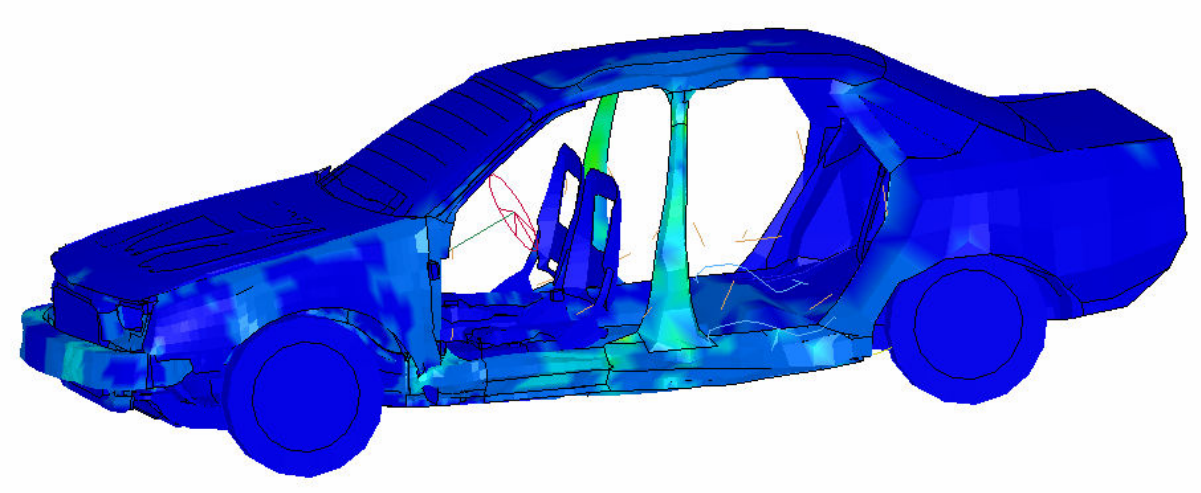

Figure 25. Deformation in the Composite B-Pillar

From figure 24, and 25, it can be seen that the deformation of the car when the present B-Pillar is used is very high. This indicates that the displacements and the accelerations sustained by the car is increased, hence increasing the injuries sustained by the occupant. In addition, it can be observed that the deformation on the composite carbon fiber B-Pillar is less, which means that the energy absorbed by the structure is high and it passes very less force onto other structures in the car. This helps in minimizing the injury criteria to as low as possible. This becomes very clear when the injury levels are studied using MADYMO.

6.6.4 Results and Discussion

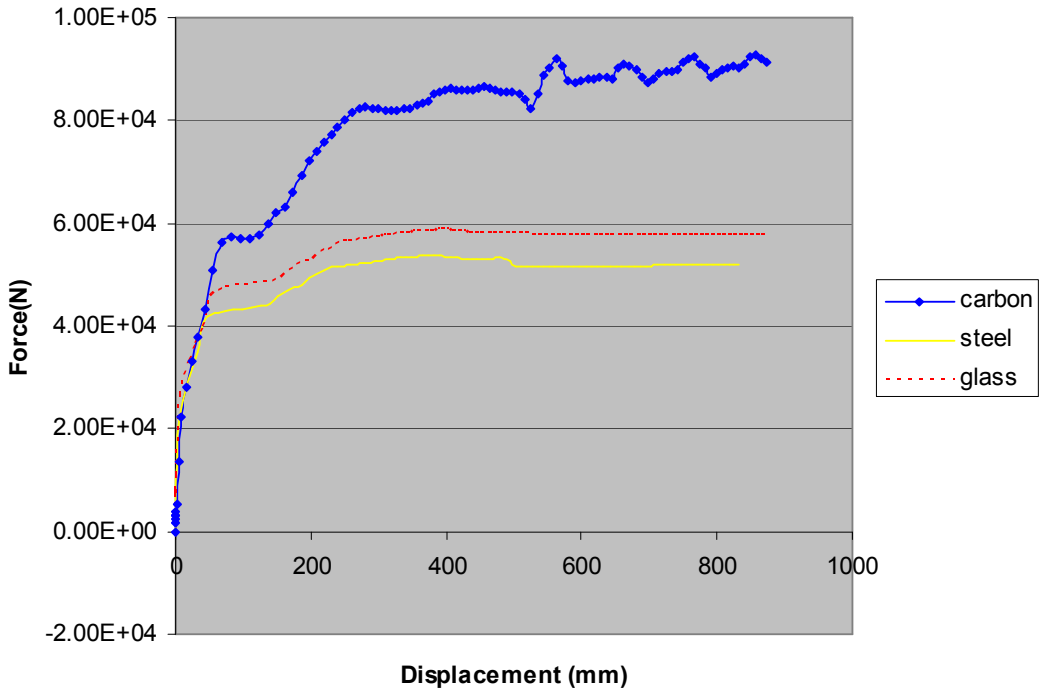

Figure 26. Force v/s Displacement for different materials

Force v/s Displacement for different materials considered can be seen from figure 26. The carbon fiber as seen has a higher ability to withstand load. The least energy absorbing material is steel as per the study. Carbon fiber is the material used for B-Pillar in this study. It can also be seen that the displacement of the B-Pillar is lesser than other materials. This means that the injury sustained by the occupant in a vehicle is reduced considerably. However, the initial peak loads of carbon fiber is high and this might induce more forces on the occupant. However, the high sustaining load offered by the carbon fiber, which absorbs higher energy thus reducing the injuries, fixes this issue. Energy v/s time is shown in figure 27. It can be seen that carbon fiber exhibits higher internal energy than any other materials, which helps in absorbing more energy.

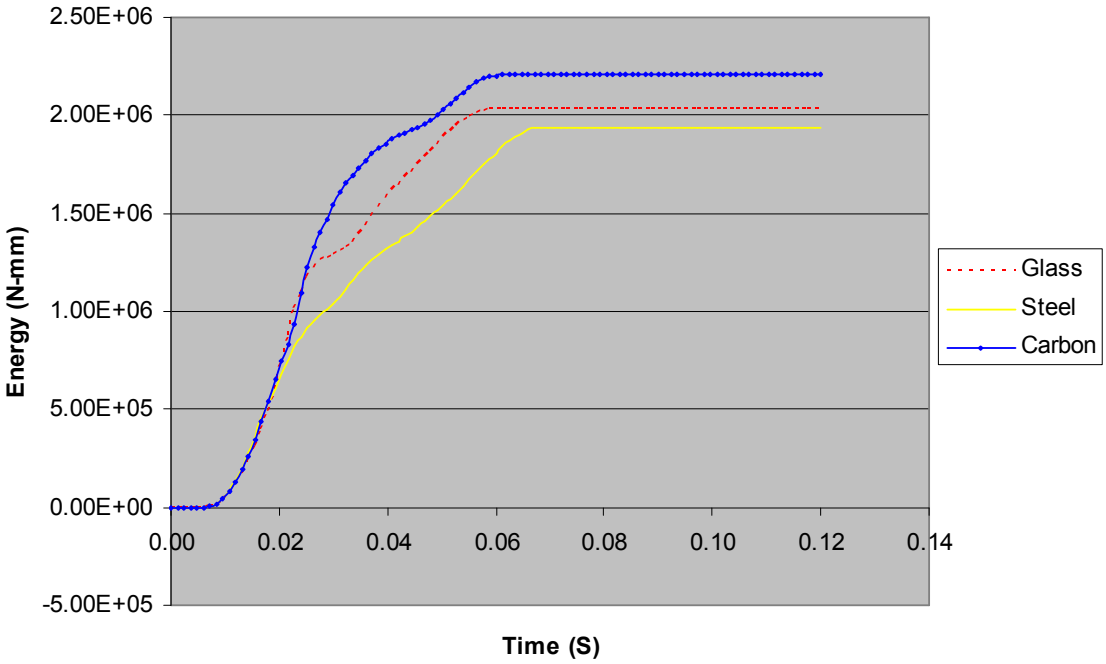

Figure 27. Energy v/s Time for different materials

TABLE 09

ENERGY ABSORPTION OF DIFFERENT MATERIALS

Material	Energy Absorption
Carbon Fiber	2.21e+6 N-mm
Glass fiber epoxy	2.01e+6 N-mm
Steel	1.84 e+6 N-mm

Table 09 shows energy absorbed by different materials. From the figure 26 and figure 27 it can be concluded that carbon fiber with orientation (0,30,-30,60,-60,90,0,90,-60,60,-30,30,0) and thickness at 3.9 mm has higher energy absorption. Therefore, these are the parameters considered when analyzing the B-Pillar.

Displacements and accelerations obtained in the side impact crash are shown in this section. In all of these displacements and accelerations curves, carbon fiber B-Pillar proves very useful.

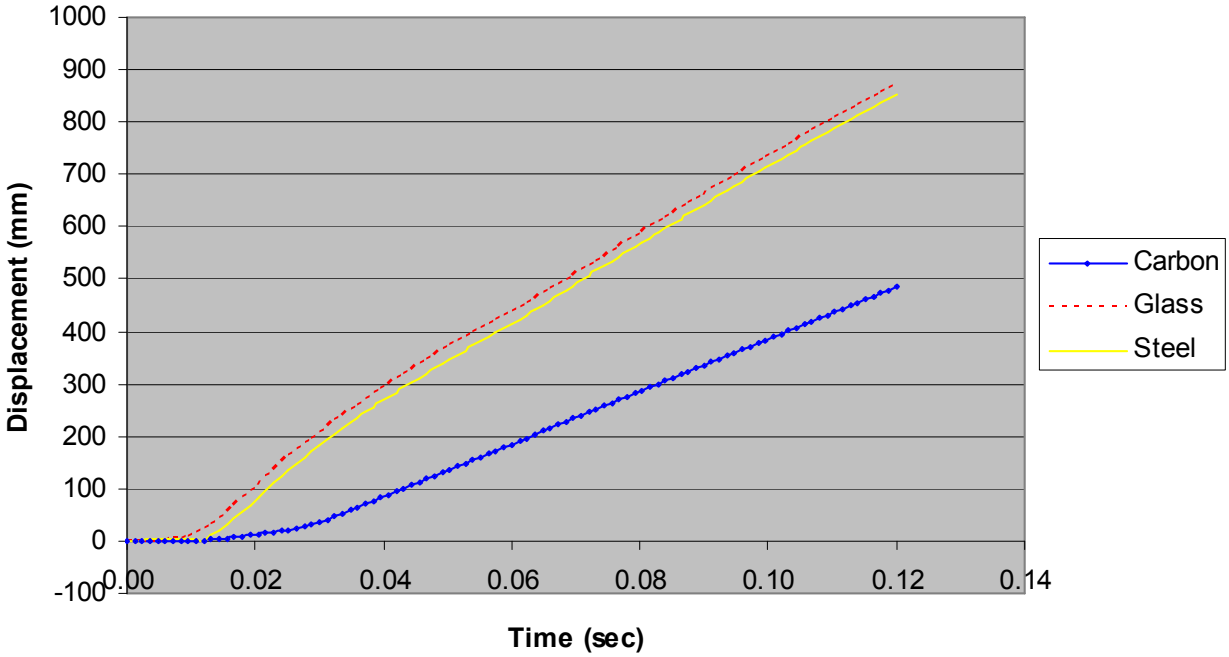

Figure 28. Displacements at the center of gravity

Figure 28 shows car's CG displacement with respect to time. Displacements in pertinent to the Present B-Pillar (Steel), Glass fiber B-Pillar (GF) and Carbon fiber B-Pillar (CF) are illustrated. The curve is self-explanatory with the Glass fiber and the present B-Pillar having almost no difference in the displacement. However, the carbon fiber B-Pillar absorbs more energy and therefore the car's displacement reduces by almost 55%. This validates the fact that carbon fibers absorb more energy and thus reduces the displacement. B-Pillar with carbon fiber shows very less displacement indicating very less intrusion into the occupant cabin. Area under the curve for carbon shows the amount of intrusion in the cabin. Intrusion in a car plays a very important role as it is directed to the safety of the occupant that is a major criterion in side impacts.

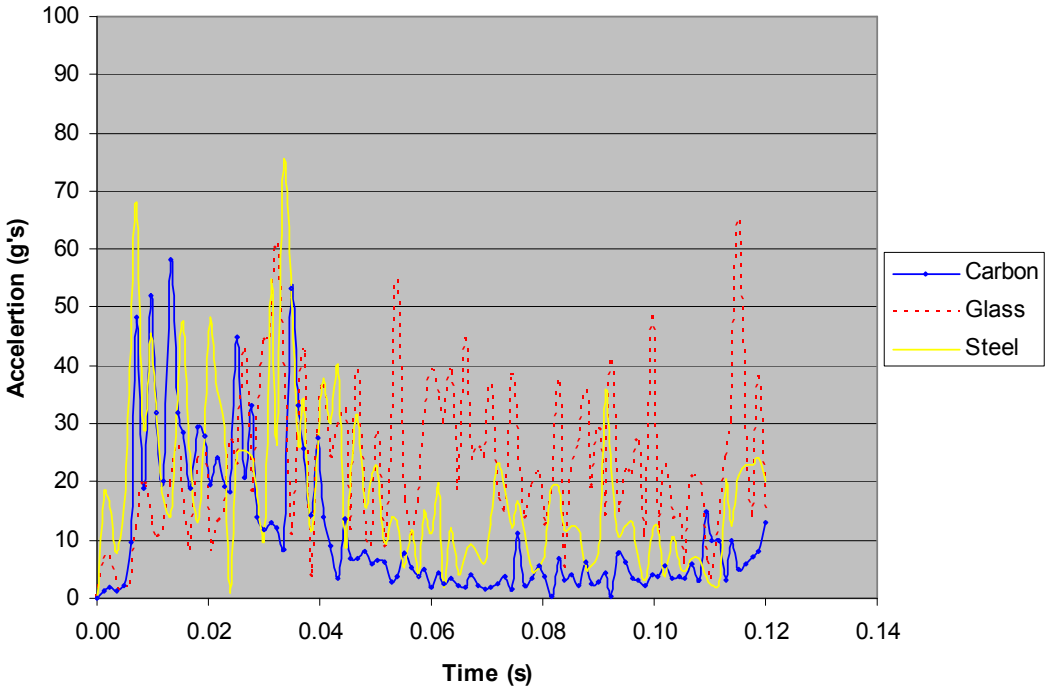

Figure 29. Acceleration of B-Pillar

Figure 29 shows the acceleration graph with respect to time. The accelerometers placed on the B-Pillar of the car shows the acceleration levels that are acting on the pillar at the time of impact. These accelerations are measured in g-forces. For a good B-Pillar the g-forces should not exceed 90g's. This is more explained in the actual crash with dummy. Here we can see that the peak acceleration of steel is very high. But carbon and glass are also very close. At the end time, acceleration of steel is 20g's and carbon is around 10g's that is lesser than steel which is in the present B-Pillar. When the peak acceleration is seen we can see that steel reaches 75g's, glass reaches 65g's and carbon is 58g's which is much lesser than steel. This shows that carbon can be used in the B-Pillar and hence injury levels can be reduced.

CHAPTER 7

OCCUPENT BIO-DYNAMIC MODELLING AND POTENTIAL INJURY

7.1 MADYMO Modeling

Crashworthiness and occupant injury simulations are often used to evaluate the effectiveness, and potential limitations of proposed test procedures and safety countermeasures. Safety of occupant is the most important issue that concerns during the design and development of vehicle.

7.2 Dummy models [21]

To simulate a human being in crash scenario MADYMO dummy models are used. Three MADYMO model types are available as shown in figure 30. These model types are Ellipsoid models, Facet models and Finite Element models.

Ellipsoid models are models that are based fully on MADYMO's rigid body modeling features. Their geometry is described by means of ellipsoids, cylinders and planes. They are the most CPU-time efficient type of models. Therefore, they are particularly suitable for concept, optimization and extensive parameter sensitivity studies.

A wide range of MADYMO ATD models are available. The standard models of the adult and child Hybrid III dummies are the 5th percentile female, the 50th percentile male, the 95th percentile male, 6-year-old child and 3-year-old child Hybrid III dummy models. The size and weight of the Hybrid III 50^{th} percentile male represents an "average" of the American adult male population. In order to cover the extremes of the American adult population two other versions of the Hybrid III have been developed, the 5^{th} percentile small female and the 95^{th} percentile large male.

Hybrid III 50th percentile dummy	EUROSID-I dummy ellipsoidal model	Standing Hybrid III 50th % dummy
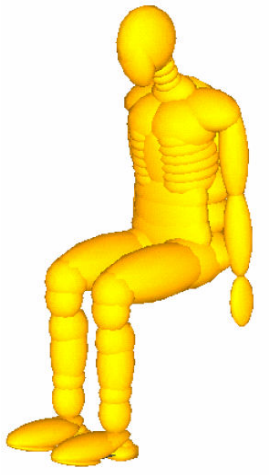	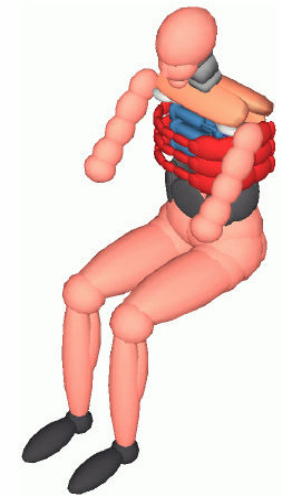	

Figure 30. Ellipsoidal dummy models [21]

Figure 30 shows the ellipsoidal dummy models. Hybrid III 50th percentile dummy is the most widely applied dummy for the evaluation of automotive safety restraint systems in frontal and side crash testing.

The EUROSID-1 Side Impact Dummy has been designed to represent a 50th percentile adult male subject during side impact crash conditions. It is used in European and Japanese side impact test procedures. The EuroSID is a lateral impact dummy which is specified in the 96/27/EG directive for the protection of motor vehicle occupants [21].

The standard Hybrid III 50th percentile dummy as shown in figure 31 has been developed for seated automotive applications. The standing Hybrid III contains some adapted parts and thereby has a wider range of application including standing and testing pedestrian accidents.

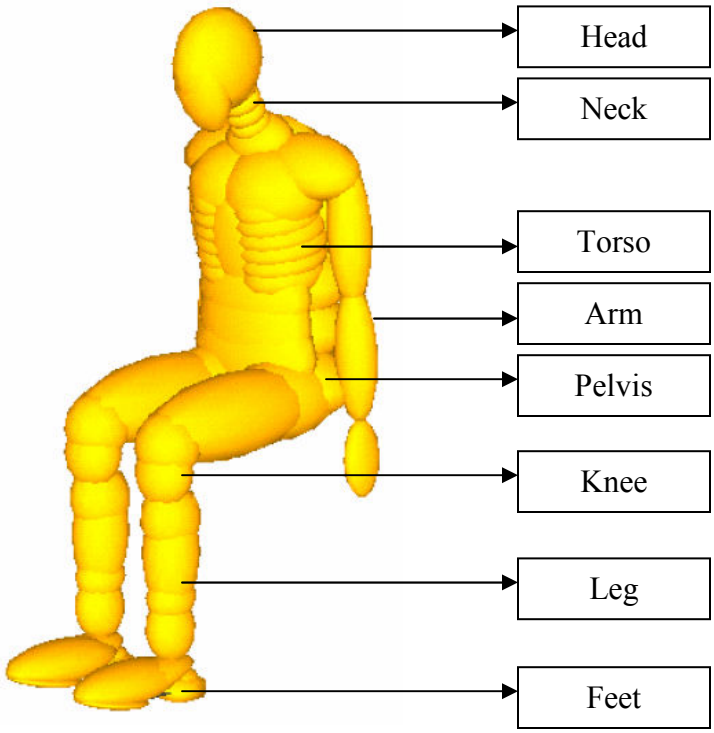

Figure 31. Hybrid III 50th percentile side impact dummy model [21]

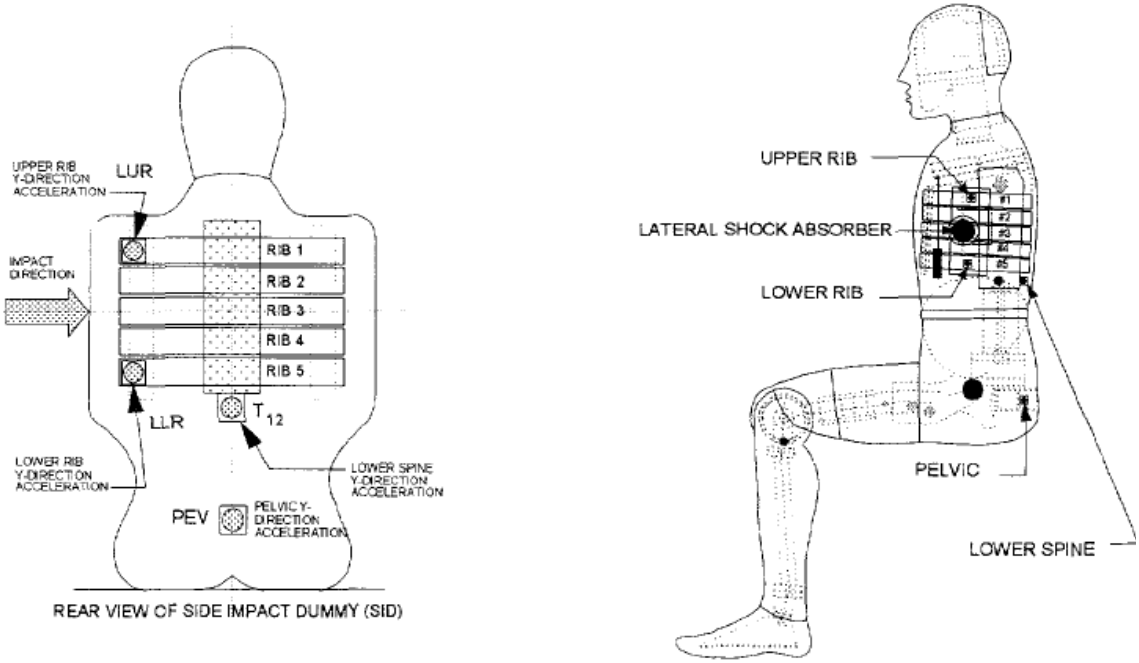

Figure 32. Rear and left side view of dummy [14]

TABLE 10

WEIGHT TABLE [14]

Factors	**Hybrid III 50th percentile male dummy**
Weight	172.3 lbs
Stature	69.0 in
Sitting Height	34.8 in

Table 10 shows the weight of the Hybrid III 50th percentile side impact dummy. The stature of the dummy is about 69 in measured from the pelvis and the sitting height is 34.8 in which can be seen from figure 32. Their geometry is described by means of ellipsoids, cylinders and planes. Segmented weights of each part from head to feet are shown in table 11.

TABLE 11

SEGMENTED WEIGHTS [14]

Part	**Weight (lb)**
Head	10.0
Neck	3.4
Upper Torso	37.9
Lower Torso	50.8
Upper Arms	8.8
Lower Arms and Hands	10.0
Upper Legs	26.4
Lower Legs and Feet	25.0
Total Weight	172.3

7.3 Dummy features

The dummy features three main parts, which are head and neck, lower torso and upper torso as shown in figure 31. The Hybrid III 50th male features a neck design that simulates the human dynamic moment / rotation, flexion, and extension response characteristics of an average size adult male. The shoulder structure was designed for improved fidelity of shoulder belt interaction [21].

7.3.1 Head And Neck

The skull and skull cap are one piece cast aluminum parts with removable vinyl skins. The neck is a segmented rubber and aluminum construction with a center cable. It can incorporate a six-axis neck transducer at the top and bottom. This accurately simulates the human dynamic moment/rotation flexion and extension response [14].

7.3.2 Upper Torso

The rib cage is represented by six high strength steel ribs with polymer based damping material to simulate human chest force-deflection characteristics as shown in figure 32. Each rib unit comprises left and right anatomical ribs in one continuous part open at the sternum and anchored to the back of the thoracic spine [21]. A sternum assembly connects to the front of the ribs and includes a slider for the chest deflection rotary potentiometer. The angle between the neck and upper torso is determined by the construction of the neck bracket which can incorporate a six-axis neck transducer. A two-piece aluminum clavicle and clavicle link assemblies have cast integral scapulae to interface with shoulder belts [14].

7.3.3 Lower Torso

A curved cylindrical rubber lumbar spine mounts provides human-like slouch of a seated person and mounts to the pelvis through an optional three axis lumbar load cell. The pelvis is a vinyl skin/urethane foam molded over an aluminum casting in the seated position as shown in figure 32. The ball-jointed femur attachments carry bump stops to reproduce the human leg to hip moment/rotation characteristics. The femur, tibia and ankle can be instrumented to predict bone fracture and the knee can evaluate tibia to femur ligament injury. The foot and ankle simulates heel compression and ankle range of motion [14]

TABLE 12

EXTERNAL DIMENSIONS FOR THE HYBRID III 50TH PERCENTILE MALE [14]

Dimension Description	**Specifications (in)**
Head Circumference	23.5
Head Breadth	6.1
Head Depth	8.0
Erect Sitting Height	34.8
Shoulder to Elbow Length	13.3
Back of Elbow to Wrist Pivot Length	11.7
Buttock to Knee Length	23.3
Knee Pivot Height	19.5

Table 12 shows the dimension of each of the parts in the Hybrid III 50th male dummy. Here the head circumference, breadth and depth are taken from a average american adult male population.

7.4 Simulation

In this study Hybrid III 50th percentile side impact dummy model is used as the reference model. Seat belts play a vital role in reducing the injuries of the occupant. Here the seat belts developed in MADYMO 601 are classified as FEM belts. These are basically the three-point belt restraint system. The width and thickness of the belt are equal to 40mm and 1mm respectively. Belts are modeled with 0.02 size tria-elements. HYSISO material is used for belts with density of 7850 kg/mm^3. Loading and unloading function for the FE belts are specified and they are as depicted in figure 33.

The contact between the dummy and the belt is defined by kinematic contacts with coefficient of friction of 0.3. The belt section of the shoulder belt is in contact with the right clavicle, the right upper arm, the neck and the collar, the left and right upper torso, the ribs, the sternum, breasts and the abdomen. The FE belt section of the lap belt is in contact with the hips, abdomen, the bottom ribs and the lower torso of the dummy. US DoT SID dummy with the planes and seatbelts is shown in figure 35.

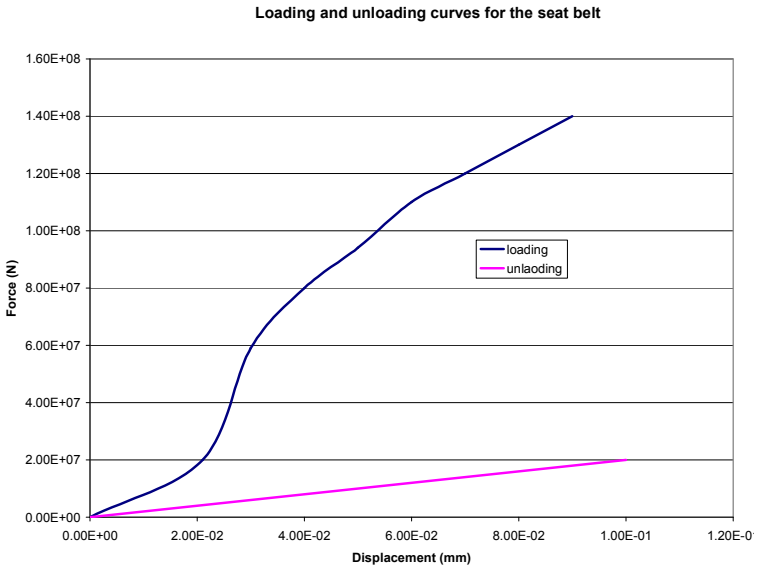

Figure 33. Loading and unloading curve for the FE belt

This dummy model created in Easi Crash MAD is merged into the car using ECD as shown in figure 34. To run the analysis, MADYMO is coupled with LS-Dyna using the simple coupling and the analysis is run for 0.1 sec. Animation sequence is shown in figure 34.

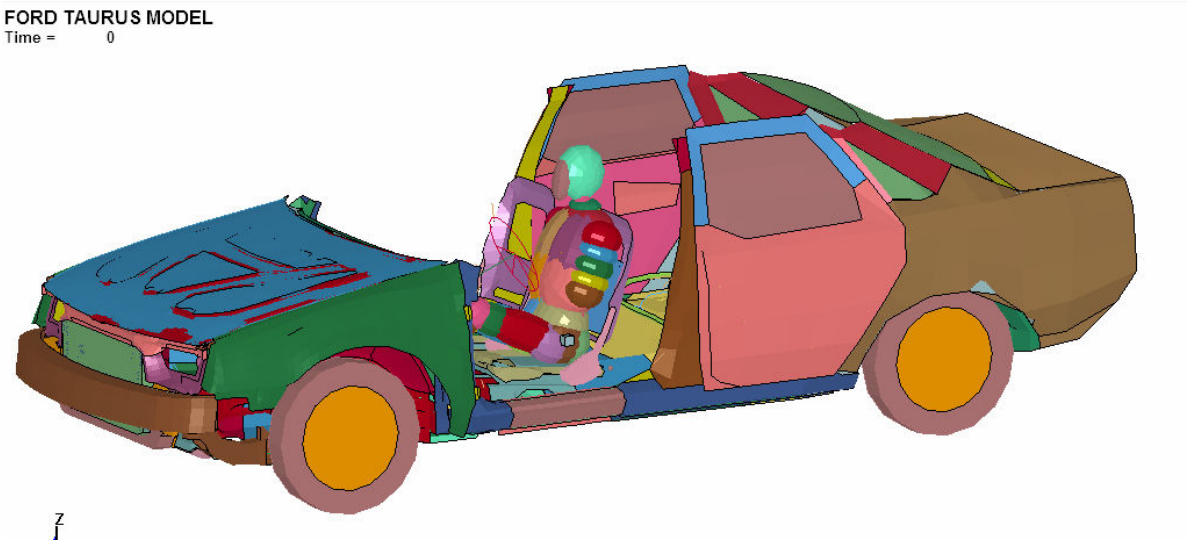

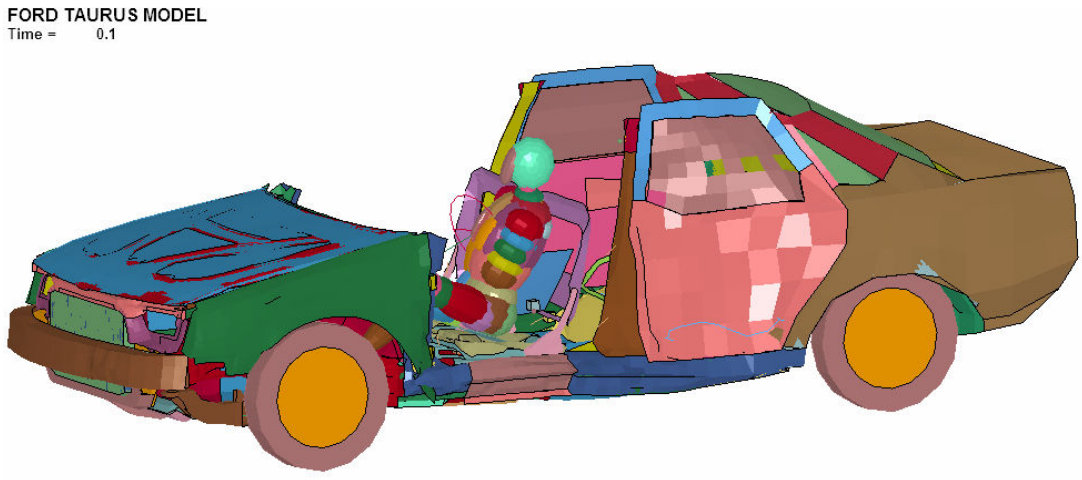

Figure 34. Dummy merged with the car

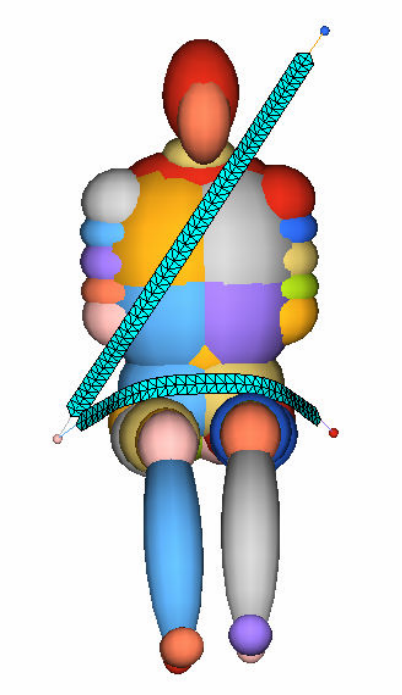

Time = 0 sec

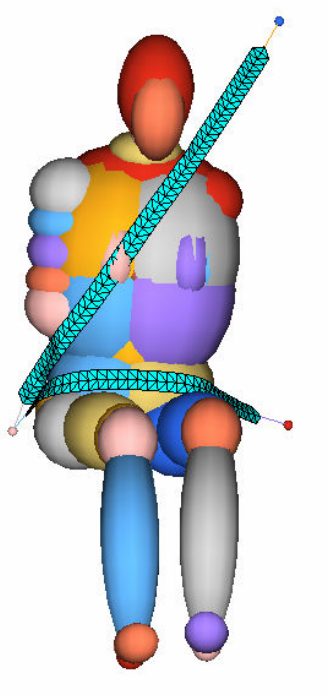

Time = 0.01 sec

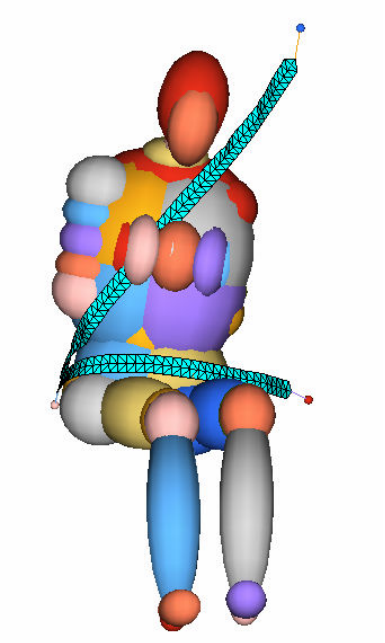

Time = 0.04 sec

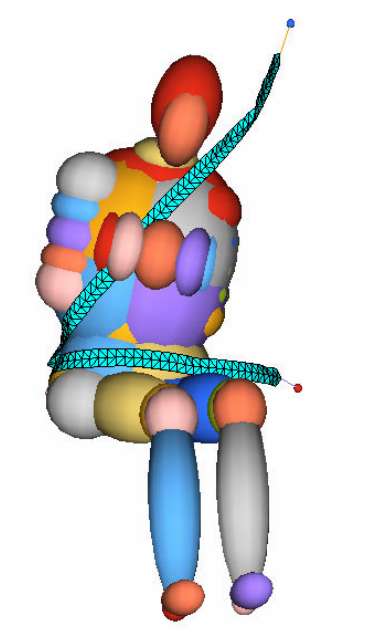

Time = 0.07 sec

Figure 35. Animation sequence of an impact analysis

7.5 Potential injuries

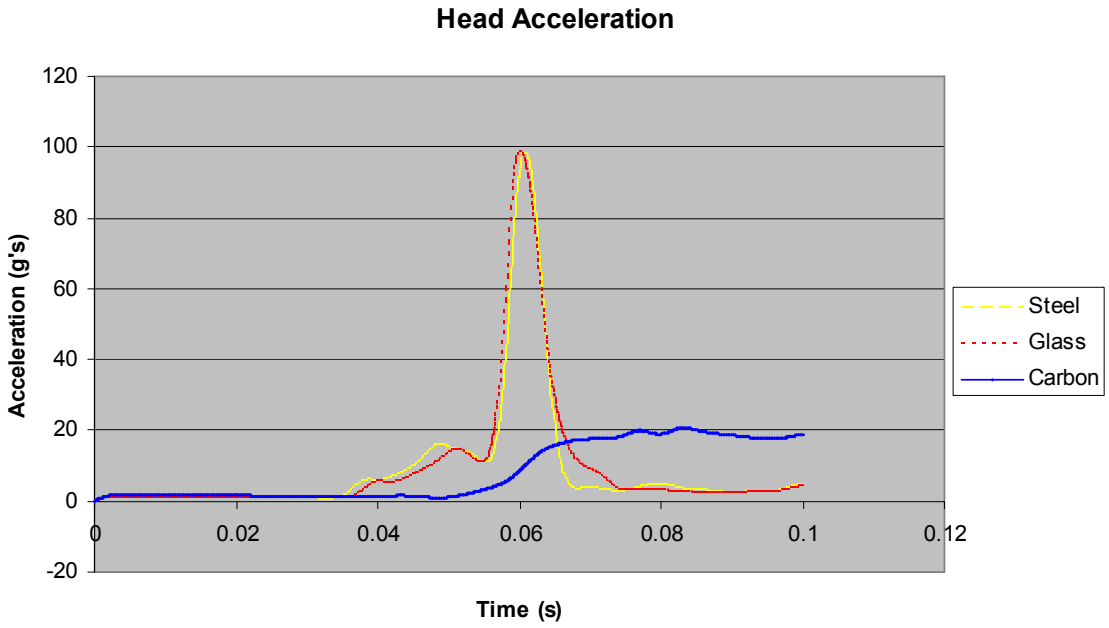

Figure 36. Head acceleration

Figure 36 shows the comparison of Head CG acceleration of driver occupant for present B-Pillar, composite B-Pillar and glass fiber. From the figure 36, it can be observed that, head CG acceleration for the car with composite fiber is lower as compared to the present and the glass fiber model. Acceleration of the present B-Pillar is around 94 g's where as the carbon fiber B-Pillar is around 20 g's. Due to this, the injury criteria HIC, reduces tremendously.

Figure 37 the comparison of Thorax Spine acceleration of driver occupant for present B-Pillar, composite B-Pillar with glass fiber and carbon fiber. Carbon fiber exhibits lesser acceleration than the other impact B-Pillar. Acceleration of the present B-Pillar is around 40 g's and the new designed B-Pillar with carbon fiber is around 10 g's.

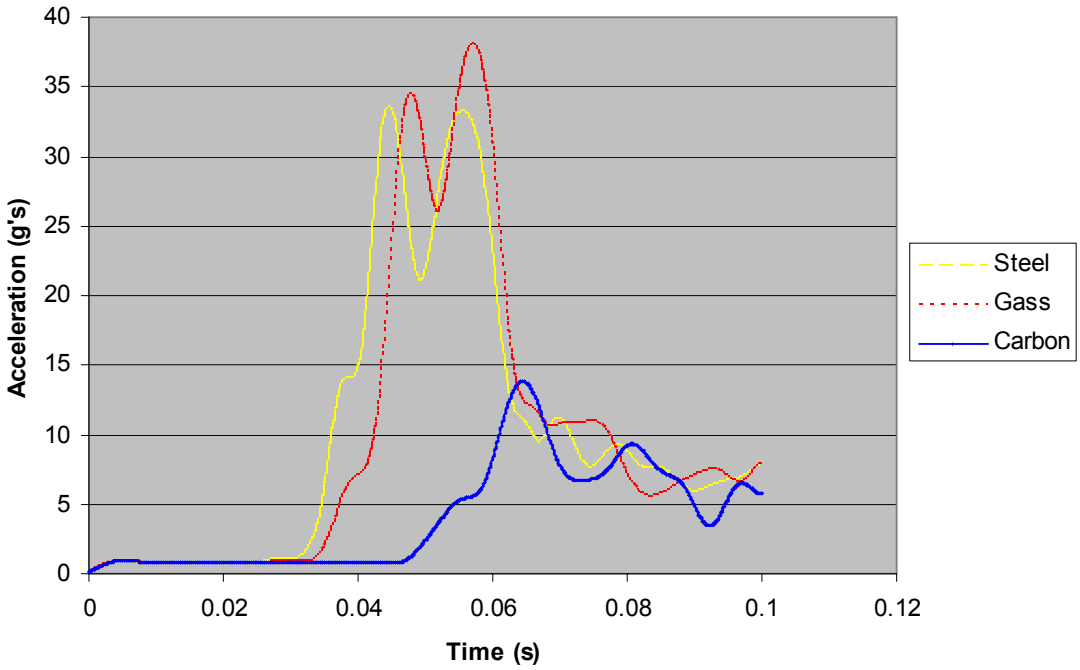

Figure 37. Thorax Spine acceleration

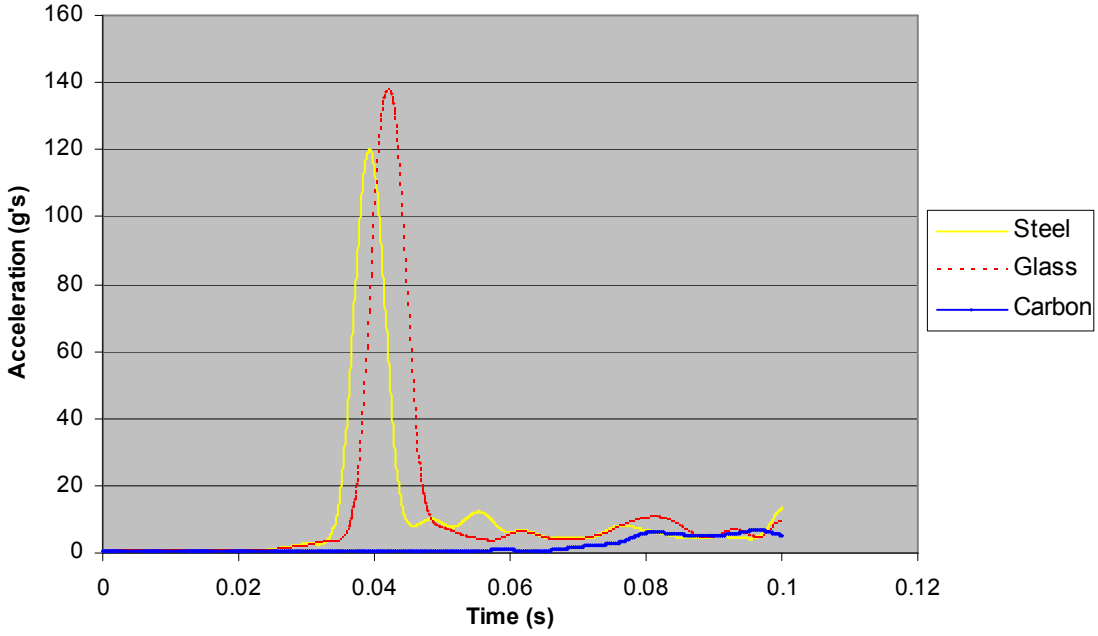

Figure 38. Pelvis acceleration

Figure 38 illustrates the curve between acceleration of pelvis regions. It can be seen that the composite fiber dominates in having lesser acceleration than the other side impact B-Pillar. This also indicates that the energy absorption of the composite fiber B-Pillar is higher and thus it helps in reducing injuries to the occupant.

TABLE 13

INJURY RATING [4]

Injury Measure	**Good**	**Acceptable**	**Marginal**	**Poor**
HIC	0-623	624-779	780-935	> 935
V*C (m/s)	0-1.00	1.01-1.20	1.21-1.40	> 1.40
TTI	0-90	91-100	101-120	>120

TABLE 14

INJURY CRITERIA CALCULATED FOR THE SIDE IMPACT CRASH

	Steel Model	**Carbon Fiber Model**	**Glass Fiber Model**
HIC	512	144	640
Head CG Acceleration (g's)	94	20	75
Thorax trauma Index	40	15	35
Pelvis Acceleration (<130g's)	120	75	100
V*C (m/s)	0.8	0.3	0.6

Table 13 shows the injury rating standards according to Insurance Institute for Highway Safety. The head injury criteria and viscous injury criteria ratings are shown

and we can see which is a good structure and a bad structure according to the values obtained.

To supplement head injury measures, the movements and contacts of the dummies' heads during the crash are evaluated. This assessment is more important for seating positions without head protection airbags, which (assuming they perform as intended) should prevent injurious head contacts. Very high head injury measures typically are recorded when the moving deformable barrier hits the dummy head during impact. Analysis of the movement and contact points of the dummies' heads during the side impact crash test is used to assess this aspect of protection.

Table 14 shows the injury criteria calculated during a side impact crash test. For head injury criteria a value of 623 is specified as the concussion tolerance level in side impacts [4]. It can be seen that the Head CG Acceleration value for the carbon fiber is very less when compared to steel and glass and is very much accepted in the field of crashworthiness. The TTI is the acceleration criterion based on accelerations of the lower thoracic spine and the ribs. The TTI can be used as an indicator for the side impact performance of passenger cars. The dynamic performance requirement, as stated in FMVSS 214 regulations of 1990, is that the TTI (d) level shall not exceed 85 g for passenger cars with four side doors and 90 g for two side doors. We can see that carbon fiber is about 15g's, which is very less than the specified standards.

The pelvic acceleration standard shows that a good structure is whose g-levels are less than 130. From table 14 we can see that the pelvis acceleration levels are very less and is very much accepted in the field of crashworthiness. When seen the viscous critera carbon fiber is again in the acceptable level.

CHAPTER 8

CONLCUSIONS AND FUTURE WORK

In this study, the objective was to investigate the use of composites as an alternative in the vehicle B-Pillar and thus help in reducing the risk of injuries on the occupant. The composite B-Pillar was tested on different grounds to find out the maximum possible energy absorbing material, orientation and thickness. A side impact B-Pillar was designed and an attempt is made to use this B-Pillar in the vehicle. FMVSS tests are conducted to find out the accelerations and the intrusion sustained by the vehicle before and after the use of composite B-Pillar. Finally, occupant kinematics was studied and discussed in detail.

The composite B-Pillar designed is tested axially and in the transverse direction. Different materials and orientation are used to find out the parameters that gives the highest possible energy absorption. By implementing the composite designed B-Pillar into the vehicle, the acceleration, displacement and the injuries sustained by the occupant was eventually reduced.

8.1 Conclusions

The following conclusions can be made:

- Composite B-Pillar absorbs more energy and hence, the deformation sustained by the B-Pillar is more, which leads to decrease in the displacement and acceleration of the car to about 55%.
- Using this B-Pillar would reduce the weight of the side impact B-Pillar to about 65%.

- Injury level reduces (70%) drastically assuring the composite B-Pillar is stronger than the present B-Pillar.
- This B-Pillar is effective in FMVSS (25% reduction in acceleration) standards.
- With the present technologies involved, this B-Pillar is easy to manufacture.
- There are no complications of adhering the composite B-Pillar to the car.
- Although the composite B-Pillar fail by buckling during impact loading, by proper design, fiber orientation and fiber matrix combination buckling failure can be reduced.

8.2 Future Work

The following recommendations for future work can be noted:

- Materials other than carbon fiber/glass fiber can be used or a combination of different composite materials can be used to strengthen the B-Pillar.
- Experimental tests can be carried out to find out the accuracy of the results obtained.
- Manufacturing though easy can be expensive, an alternative to reduce the manufacturability can be figured out.
- Extensive MADYMO analysis dealing with the Neck Injuries, viscous injury response and so on can be studied to know the effectiveness of the composite B-Pillar.

REFERENCES

REFERENCES

[1] D.B. Miracle, S.L. Donaldson, "Introduction to Composites". *Journal of Composite Materials*, vol.34, pp.200-215, 1995.

[2] Farley, G.L.,and Jones, R.M., "Crushing Characteristics of Continuous Fiber-Reinforced Composite Tubes," *Journal of Composite Materials*, Vol.26, No.1, pp. 37-50, 1992.

[3] Matzenmiller, A., and Schweizerhof, K., "Crashworthiness Simulations of Composite Structures-A First Step with Explicit Time Integration," *Nonlinear Computational Mechanics- A State of the Art, Springer Verlag*, New York, 1991.

[4] IIHS, "*Crashworthiness Evaluation Side Impact Crash Test Protocol (version III)",* Insurance Institute for Highway Safety, April 2004.

[5] R Adam, H., Patberg, L., Philipps, M. & Dittmann, R., "Testing of New Composite Side Door Concepts", Proceedings of the 1998 SAE International Congress & Exposition, SAE Special Publications, Vol. 1320, pp. 23-30, 1998.

[6] Philipps, M., Patberg, L., Dittmann, R., Henrik, A., "Structural Analysis and Testing of Composites in Automotive Crashworthiness Application", SAE Special Publications, Safety and Material Test Methodologies, v 1320,pp. 97-101, 1998.

[7] Jacob, C.G., Fellers, F.J, Simunovic, S., Starbuck, J.M., "*Energy Absorption in Polymer Composites for Automotive Crashworthiness*", 1996.

[8] Fleming, D.C., "*The Energy Absorption of Graphite/Epoxy Truncated Cones*," M.S. Thesis, Department of Aerospace Engineering, University of Maryland, College Park, 1991.

[9] Federal Motor Vehicle Safety Standards (FMVSS) No.214 "*Side Impact Protection. U.S Department of Transportation"*, 1995.

[10] Farely, G.L., "Energy Absorption of Composite Materials", *Journal of composite Materials*, Vol. 17, pp. 267-279, 1983.

[11] Philipps, M., Patberg, L., Dittmann, R., "*Fiber-reinforced Composites in the Car Side Structure*". SAE Special publications, 981140, Safety and Material Test Methodologies, v 1420, pp 105-107, Feb, 1998.

[12] Cheon, Seong Sik, "*Composite Side-door Impact B-Pillar for Passenger Cars*", Vol. 38, No. 1-4, pp. 229-239, 1997.

[13] Marklund, P.O., Nilson, L., "Optimization *of a Car Body Component Subjected to Side Impact*", Vol. 12, pp.100-105, 1999.

[14] Cing-Dao, Dhafer Marzougui, "*Development of a 50th Percentile Hybrid III Dummy Model",* pp. 1-10, 2003.

[15] Joseph N. Kanianthra, Glen C.Rains and Thomas J. Trella. "*Strategies for Passenger Car Design to Improve Occupant Protection in Real World Side Crashes*", 1994.

[16] Nguyen, Q.M.,Elder J.D., Bayandor, J., Thomson, S.R., Scott, L.M., "*A review of Explicit Finite Element Software for Composite Impact Analysis*",1999.

[17] S. Ramakrishna and H. Hamada, "*Energy Absorption Characteristics of Crash worthy Structural Composite Materials*", Engineering Materials, Vol. 141-143 pp.585-620, 1998.

[18] Thornton, P.H., "*Energy Absorption in Composite Structures*", Journal of Composite Materials, Vol. 13, pp. 247-262, 1979.

[19] Mamalis, A.G.Robinson, M.Carruthers, "*The Energy Absorption Properties of Composite Materials*", Composite Structures Vol. 37, pp 109-134, 1997.

[20] LS-Dyna User's Manual Version 970.

[21] MADYMO User Manual Version 6.0.1.

[22] Schweizerhof, K., Weimar, K., Th. Munz, Rottner, T., "*Crashworthiness Analysis with Enhanced Composite Material Models in LS-DYNA Merits and Limits*", 1997.

[23] Johnson, A.F.,and Kohlgrüber, D., *" Modelling the Crash Response of Composite Aircraft Structures*," European Conference on Composite Materials Naples, Italy, Vol. 1, pp. 283- 290, 1998.

[24] Honnagangaiah.K, "*Design and Evaluation of Car Front Sub frame Rails in a Sedan and its Corresponding Crash Injury Response*", M.S. Thesis, Department of Mechanical Engineering, Wichita state university, 2006.

[27] Sheshadri, A., "*Design and Analysis of a Composite Beam and its use in Reducing the Side-impact Injuries in a Sedan*", M.S. Thesis, Department of Mechanical Engineering, Wichita State University , Wichita, 2006.

[28] "*National Highway Traffic Safety Administration Annual Report*", 2005.

[29] Hansun Chan, James.R.Hackney, Richard. M. Morgan, "*An Analysis of Side Impact Crash Data",* Conrad Technologies, pp. 0-12, 1998.

APPENDIX

APPENDIX

TABLE 15

GLASS FIBER PROPERTIES

Property	Value	Units
Density	1.97E-06	Kg/mm^3
Ply longtitudinal modulus	45.84	Gpa
Ply transverse modulus	17.50	Gpa
Ply poisson's ratio	0.26	-
Ply shear modulus in plane	8.63	Gpa
Ply transverse modulus parallel to fiber direction	6.57	Gpa
Ply transverse modulus perpendicular to fiber direction	8.63	Gpa
Ply longitudinal tensile strength	1.12	Gpa
Ply longitudinal compressive strength	0.9	Gpa
Ply transverse tensile strength	0.03	Gpa
Ply transverse compression strength	0.13	Gpa
Ply shear strength	0.07	Gpa

APPENDIX (Continued)

TABLE 16

CARBON PROPERTIES

Property	Value	Units
Density	1.58E-06	Kg/mm^3
Ply longtitudinal modulus	142	Gpa
Ply transverse modulus	10.3	Gpa
Ply poisson's ratio	0.27	-
Ply shear modulus in plane	7.12	Gpa
Ply transverse modulus parallel to fiber direction	3.15	Gpa
Ply transverse modulus perpendicular to fiber direction	7.12	Gpa
Ply longitudinal tensile strength	1.83	Gpa
Ply longitudinal compressive strength	1.09	Gpa
Ply transverse tensile strength	0.05	Gpa
Ply transverse compression strength	0.22	Gpa
Ply shear strength	0.07	Gpa